



## Improving archaeomagnetic interpretations by reusing magnetically oriented samples for micromorphological analysis

Ada Dinçkal<sup>a,b,c,\*</sup>, Ángela Herrejón Lagunilla<sup>c</sup>, Angel Carrancho<sup>d</sup>,  
Cristo M. Hernández Gomez<sup>a</sup>, Carolina Mallol<sup>a,b</sup>

<sup>a</sup> Area de Prehistoria, Arqueología E Historia Antigua, Departamento de Geografía E Historia, Facultad de Humanidades, Universidad de La Laguna, Campus de Guajara, 38071, La Laguna, Santa Cruz de Tenerife, Spain

<sup>b</sup> Archaeological Micromorphology and Biomarkers (AMBI Lab), Instituto Universitario de Bio-Organica Antonio Gonzalez (IUBO), Universidad de La Laguna, Apartado 456, 38206, La Laguna, Santa Cruz de Tenerife, Spain

<sup>c</sup> Laboratorio de Paleomagnetismo, Dpto. Física, Escuela Politecnica Superior, Edificio A1, Universidad de Burgos, Avda. Cantabria S/N 09006, Burgos, Castile and Leon, Spain

<sup>d</sup> Area de Prehistoria, Dpto. Historia, Geografía y Comunicación, Laboratorio de Prehistoria, Edificio I+D+I, Universidad de Burgos, Plaza Misael Banuelos S/N. 09001, Burgos, Castile and Leon, Spain

### ARTICLE INFO

#### Keywords:

Geoarchaeology  
Soil micromorphology  
Archaeomagnetism  
Archaeological science  
Archaeological methodology

### ABSTRACT

Here we present a novel approach that combines soil micromorphology with the analysis of magnetically oriented samples to improve the interpretation of archaeomagnetic results. The aim is to test whether irregular archaeomagnetic data can be examined with micromorphological soil analysis in a single sample methodology, allowing said archaeomagnetic data to contribute to more meaningful archaeological interpretation. Experimental work included reusing oriented magnetic samples previously treated with sodium silicate resin, which were then re-impregnated with polyester or epoxy resins to produce thin sections. Initial experimentation was conducted to understand the potential effects of sodium silicate treatment on the optical and mechanical qualities of the thin sections. When no significant optical anomalies were identified, the methodology was tested using samples gathered from hearths at level X (ca. 52 ky BP) at the Middle Palaeolithic site of El Salt, Spain. Thin section analysis was conducted on archaeological hearth samples to identify syn- and post-depositional processes influencing the magnetic data. Micromorphological analysis of magnetic samples can identify the causes of anomalous magnetic direction, attributing them to specific sedimentary features rather than sampling or measurement errors. Discrepancies in magnetic signatures are linked to the presence or absence of certain combustion layers, such as black and white layers, as well as the impact of bioturbation and mechanical deformation. This integrative approach improves the interpretive potential of archaeomagnetic studies by not only validating the magnetic data as representative of the deposit but also providing a visual understanding of the sedimentary structure creating the magnetic signature. Our findings advocate for the routine inclusion of thin section inspection in archaeomagnetic research, particularly when dealing with complex sedimentary sequences and ambiguous magnetic data.

### 1. Introduction and background

The analysis of magnetically oriented samples is fundamental in archaeomagnetism, providing detailed information on the Earth's magnetic field within human-derived or associated sediments, as well as the processes that affect them after deposition (Tarling 1975; Carrancho and Villalán 2011; Carrancho et al., 2012; Kapper et al., 2014; Shakh-Gross et al., 2018; Herrejón Lagunilla et al., 2019; Bradák et al.,

2020). It is often used for archaeological chrono-sciences (Tarling 1975; Carrancho et al., 2016a; Herries and Adams, 2013; Dirks et al., 2017; Carrancho et al., 2016b; Zeigen et al., 2019); and most recently, was employed to determine the minimum time elapsed between several combustion features at El Salt (Herrejón Lagunilla et al., 2024), offering a novel archaeological method for quantifying diachrony in a single stratigraphic unit. The veracity of those results depends on being able to reliably reconstruct the magnetic signature recorded in the sediment,

\* Corresponding author.

E-mail address: [adinckal@ull.edu.es](mailto:adinckal@ull.edu.es) (A. Dinçkal).

<https://doi.org/10.1016/j.jas.2024.106081>

Received 1 July 2024; Received in revised form 5 September 2024; Accepted 6 September 2024

Available online 14 September 2024

0305-4403/© 2024 The Author(s). Published by Elsevier Ltd. This is an open access article under the CC BY license (<http://creativecommons.org/licenses/by/4.0/>).

which can be affected by numerous environmental and anthropogenic processes, as well as errors from excavation or laboratory procedures. Micromorphological analysis can visually identify pivotal components of a stratigraphic unit such as bioturbation; redoximorphic features or mechanical reworking, that can influence the magnetic characteristics and cause anomalous magnetic data. This work builds upon prior research (Dinçkal et al., 2024), which utilized environmental and rock magnetic analysis to aid micromorphological interpretations. Comparatively, here we utilize thin section analysis to significantly enhance the understanding of sedimentary features relating to archaeomagnetic results while also distinguishing laboratory-induced magnetic anomalies from those that are characteristic of the sediment. In this study we aim to understand irregular archaeomagnetic data through the confluence of these methodologies, soil micromorphology and archaeomagnetism, in a single-sample analysis to help improve interpretations of syn- and post-depositional processes in archaeological deposits.

Soil micromorphology, a key geoarchaeological analytical method, explores syn and post-depositional processes within archaeological sedimentary sequences. Micromorphological analysis can identify the

sequence in which anthropogenic, geogenic, biogenic, and environmental processes have occurred to create the archaeological deposit, providing a strong framework for interpreting the history of the deposit's formation and post-depositional alteration (Karkanas and Goldberg 2018; Goldberg and Berna 2010). Recent advancements have focused on integrating micromorphology with other methods of geoarchaeological research, aiming to improve the utility and interpretative potential of the geoarchaeological field in general (e.g., Mentzer 2017; Berna 2017; Miller et al., 2016). This includes geochemical analysis (see Weiner et al., 1993; Weiner et al., 2002; Karkanas et al., 2000; Miller et al., 2016; Berthold and Mentzer, 2017; Mentzer 2017; Wilson 2017), biomarker and lipid analysis (e.g., Mallol et al., 2013; Connolly et al., 2019; Leierer et al., 2019; Rodríguez De Vera et al., 2020; Tomé et al., 2024), ancient DNA (Massilani et al., 2022) and rock magnetic analysis (Ozán et al., 2019; Reidsma et al., 2021; Dinçkal et al., 2022, 2024) to name a few examples.

At El Salt, extensive archaeomagnetic analysis has been conducted in the framework of numerous projects (published projects; Leierer et al., 2020; Herrejón Lagunilla et al., 2024), however consistently hearths

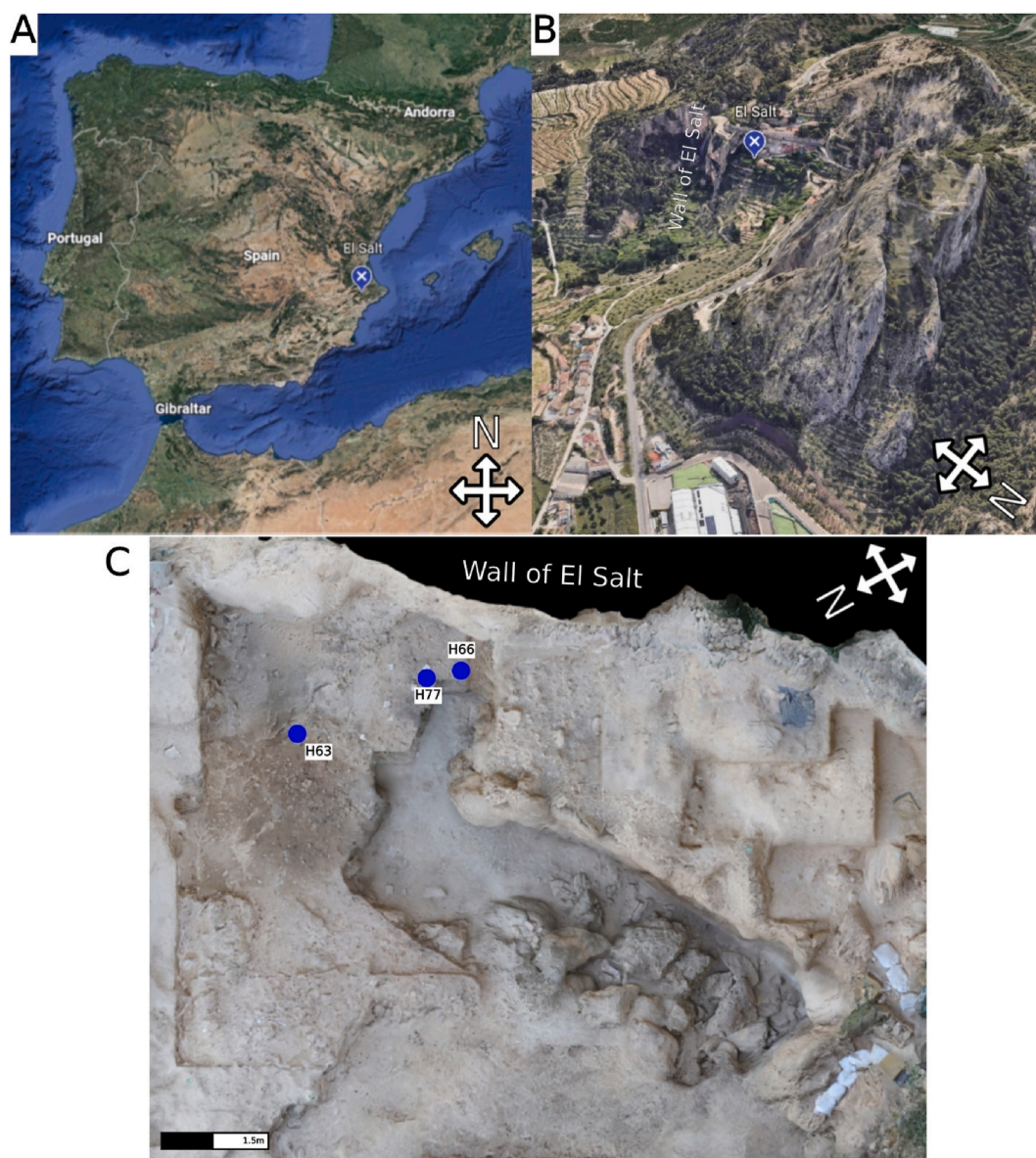


**Fig. 1.** A) Location of El Salt on the Iberian Peninsula. Image taken from Google Earth. B) Aerial view of El Salt and surrounding area. Image taken from Google Earth. C) Overhead view of El Salt with the location of the hearths studied in this work.

with magnetic properties which are anomalous to the archaeological or sedimentary context have been left out of their respective studies. Sampling for magnetically oriented archaeomagnetic analysis target archaeological combustion features, often removing the easily disturbed white layers to take a palm sized sample of the stable carbonized black layers which are likely to have maintained a record of the earth's magnetic field (Tauxe 2010; Herrejón Lagunilla et al., 2024). Understanding what sedimentary features lead to magnetic data anomalous to its context is important to discerning whether the samples reflect the actual sedimentary fabric or is a byproduct of laboratory error. Furthermore, it can be crucial for comprehending the syn and post depositional processes affecting the magnetic signature of these hearths as well as retrieving new interpretive data associated with sedimentary or anthropogenic processes. Applying micromorphological analysis directly to these samples can help address these issues. In this study we adopt such a novel approach. First, mechanical experiments were conducted to identify the optimal way to manufacture thin sections from magnetically oriented hand block samples. This included tests to identify any potential changes to optical qualities brought on by crystal growths, dyeing of the resin or sediment, or chemical reaction to the micromorphological resins that may have been formed as a byproduct of the use of sodium silicate solution in the original magnetic sampling process. Afterward, we utilize previously archived archaeological samples from three of El Salts hearths; two from previously unpublished hearths with anomalous archaeomagnetic data as well as Hearth H77 (Leierer et al. (2020; Dinçkal et al., 2024).

Archaeological samples for this study come from the site of El Salt (38°41'14"N 0°30'32"W), located in Alcoi, Spain (Fig. 1). A significant Middle Palaeolithic Neanderthal site with deposits dating from about 60.7 to 45.2 thousand years ago (Galván et al., 2014). Research at El Salt utilizes deeply integrated multi-method and proxy approaches. Studies have focused on different aspects of the archaeological context: lithic production (Mayor et al., 2022, 2024; Bencomo et al., 2023), bones of animals introduced by humans (Pérez et al., 2019; Pérez, 2023) and other naturally occurring animals (Marquina et al., 2020, Marquina-Blasco et al., 2022; Marin-Monfort et al., 2021; Fagoaga et al., 2018, 2019), charcoal and seeds (Vidal-Matutano et al., 2017, 2018), in order to understand the characteristics and variations of human behavior and its environmental setting, with special emphasis on methodological strategies to approach the dissection of palimpsests (Machado and Pérez, 2016; Machado et al., 2017; Pérez et al., 2020; Mayor et al., 2020, 2022).

Geoarchaeological approaches have included the examination of archaeological hearths, stratigraphic units containing combustion residues, and the study of ancient magnetic signals from burnt materials (Mallol et al., 2013; Leierer et al., 2019; Herrejón Lagunilla et al., 2019; Leierer et al., 2020; Dinçkal et al., 2024; Herrejón Lagunilla et al., 2024). Research into ancient biomarkers, particularly lipids, has provided insights into the substances Neanderthals might have used or consumed (Mallol et al., 2013; Leierer et al., 2019, 2020; Sistiaga et al., 2014). Additionally, the analysis of ancient DNA (aDNA) from the site has opened new avenues for understanding Neanderthal biology and diet through the innovative integration of soil layer analysis and biomolecule studies (Rampelli et al., 2021). Due to the high level of integration of archaeological scientific methods, El Salt is an ample proving ground for our methodology. With the growing capabilities of archaeomagnetic research, this paper combined with our previous research, also on material related to El Salt (Herrejón Lagunilla et al., 2019; Leierer et al., 2020; Dinçkal et al., 2024), reinforced the benefits of integrating analysis between differing veins of magnetic data with micromorphological interpretations.

## 2. Methodology

### 2.1. General explanation

Before we could begin to answer issues relating to anomalies in archaeomagnetic data, at El Salt, we had to conduct initial experimental work to evaluate the optical qualities of samples previously prepared for archaeomagnetic analysis. The initial preparation of samples for magnetic analysis commonly requires the impregnation of the sample by a solution of Sodium Silicate ( $\text{Na}_2\text{Si}_3\text{O}_7$ , referred to as NaSi) and water. The efficacy of preparing thin sections from these samples is not known so far. Producing a standard micromorphological thin sections requires using resin—commonly polyester thinned with styrene, or with epoxy—that is slow-hardening to fully consolidate the sample, while robust enough to preserve sedimentary structures, and pliable for grinding to 30  $\mu\text{m}$ . Such thickness ensures that the resin's optical properties are suitable for analysis by transmitting light microscopy. Detailed description on the methodology and application of micromorphology can be found in Miller et al. (2016), as well as Goldberg and Berna (2010) for theoretical importance. We focused on the mechanics of re-impregnating NaSi-impregnated magnetic samples with either epoxy or polyester resins and making sure optical anomalies were not present or interfere with the analysis of those thin sections.

Experimental work was conducted to study potential optical effects on the final sample. Initial experiments included re-impregnating NaSi samples with both polystyrene solution and epoxy. Mechanical tests were conducted to identify the utility of producing samples (Experiment 1: Mechanical Test Thin Sections), followed by a controlled experiment from sediment samples (Experiment 2: Controlled Experiment) to compare optical qualities. Finally, analysis on archived archaeological material, from El Salt, with previously measured magnetically oriented samples was conducted to demonstrate the utility of performing micromorphological analysis on magnetic samples (Experiment 3: Archived Archaeological Material). Detailed methods are as follows.

### 2.2. Experiment 1 - Mechanical test thin sections

The objective of these initial experiments was to assess the feasibility of producing thin sections from samples previously impregnated with NaSi and making sure that there were no apparent optical anomalies in the final thin section. For this purpose, a selection of samples was utilized from the archives of the Paleomagnetism Laboratory at the University of Burgos. These samples encompassed a diverse array of materials, from calcareous sand to ceramic fragments and experimental furnace deposits. 9 samples were turned into thin sections after being re-impregnated with either polyester ( $n = 6$ ) resin or epoxy resin ( $n = 3$ ; Table 1 for a list of original samples turned into Thin Sections). Preliminary testing involved saturating samples with only sodium silicate until they solidified. However, it was observed that sodium silicate samples were too brittle for thin section production, leading to the dismissal of this treatment. Additionally, partial re-impregnation would always occur due to the use of epoxy glue during the mounting of samples to glass for thin section production, making sole sodium silicate impregnation unnecessary. Thus, for the epoxy treatment, samples were submerged in epoxy resin within small containers and left to harden over a 24-h period. The polyester resin samples were treated with a mix consisting of 70% polyester and 30% styrene, with a hardening agent added at a concentration of less than 1%, following standard practices in micromorphological analysis (Miller et al., 2016). These samples were then affixed to glass slides with epoxy glue and meticulously ground to a thickness of 30  $\mu\text{m}$  before undergoing analysis under a transmitted light microscope to evaluate the optical properties of the thin sections. Initial manufacturing of samples for magnetic analysis was conducted at the Paleomagnetism Laboratory of the University of Burgos, while re-impregnation, thin section production and analysis was carried out at the University of La Laguna.

**Table 1**

Original archived samples which were successfully turned into thin sections after re-impregnation with organic resin. Sample code denotes the project reference number for the samples. All impregnations were conducted by submerging the sample into the resin no matter the resin used. Samples were created from leftover material from prior magnetic research which no longer had utility for any magnetic or other analysis.

Sample Code	Re-impregnation Resin	Content of Sample
MagMa-NSE7E1	Epoxy	Originally unconsolidated. Composed of silt sized to fine-sand sized aggregates of clay or micritic sands. Massive structure with calcareous aggregates and discrete nodules of coalesced groundmass.
MagMa-NSE7N2	Polyester	Originally unconsolidated. Composed of silt sized to fine sand sized aggregates of clay or micritic sands. Massive structure with calcareous aggregates and discrete nodules of coalesced groundmass.
MagMa-NSE7NE3	Epoxy	Originally unconsolidated. Composed of silt sized to fine sand sized aggregates of clay or micritic sands. Massive structure with calcareous aggregates and discrete nodules of coalesced groundmass.
Magma-NSE6N11	Polyester	Large fragment of tufa with some clay rich groundmass intermixed.
Magma-NSE6N12	Polyester	Large fragment of tufa with some clay rich groundmass intermixed.
Magma-NSE1N15	Polyester	Remnant of a medieval hearth. Coarse sand-sized quartz rich inside a matrix of rubified clay.
Magma-NSE9N16	Polyester	Black layer and white layer remnant of a paleolithic Hearth. Presence of bone and burnt limestone.
MagMa-NSE14N18	Polyester	Heavily stratified ash rich layer and organic rich layer from an experimental fumier deposit.
Magma-NSE7N26	Epoxy	Composed of silt to fine sands sized aggregates of clay or micritic sands. Massive structure with calcareous aggregates and discrete nodules of coalesced groundmass.

### 2.3. Experiment 2 - Controlled experiment

Experiment 2 was carried out to ensure there were no significant optical differences between standard micromorphological thin sections and those produced after the initial treatment of the sample with sodium silicate solution. To secure accurate comparisons across all types of impregnations, two sets of sediment samples were collected from modern substrates surrounding El Salt. The first set originated from lithified calcareous sediment atop the site. The second set was harvested from the organically rich topsoil adjacent to El Salt. Each set comprised two blocks, approximately 10 × 10cm and 5 cm deep, labelled as A and B. Block A from both sets was initially magnetically oriented, then submerged in sodium silicate solution for 1 h before being left to dry. Afterward, they were reinforced by being covered in plaster and then cut into slabs. This process aligns with the standard methodological practice to produce magnetic handblocks. Samples labelled A.1 were impregnated with a 70% polyester to 30% styrene mixture, while samples labelled A.2 underwent overnight impregnation with epoxy resin. These samples were then ground into thin sections by Wagner Petrographic LLC. Block B were produced according to standard micromorphological manufacturing practices, impregnated with polystyrene solution, and then processed into thin sections by Wagner Petrographic LLC, Utah, USA.

In the second experiment we consider a total of 6 thin sections, 3 from each type of material (lithified calcareous sediment and rich topsoil) undergoing a standard micromorphological treatment, or a NaSi mixed with micromorphological resin treatment. Thin sections analysis focusing on their optical qualities was conducted with a transmitting light microscope at the Archaeological Micromorphology and Biomarker

(AMBI) Laboratory at the University of La Laguna, Spain.

### 2.4. Experiment 3 - Archived archaeological material

Experiment 3 includes the analysis of three hearths from Unit X at El Salt (Alcoi, dated to between 60 and 45ka): H63, H66 and H77. **Hearth 63** (Fig. 1C), found in Stratigraphic Unit Xb, is a single combustion feature that is likely disturbed post-depositionally as evidence by a diffuse contact between the edges of its black layer and the surrounding sediments. The centre of the hearth contained a calcined limestone pebble (Fig. 3A), and the excavation of the hearth consisted of extracting sediment from the black layer with noted absence of the white layer in much of the hearth. Two archaeomagnetic blocks were taken from this hearth. Archaeomagnetic sample H63-1 was taken from the periphery of the hearth, and H63-2 was taken from the centre of the hearth from beneath the limestone pebble (Fig. 3A). **Hearth 66** (Fig. 1C) is a heavily disturbed hearth. During excavation, small, frequent interstratifications of silty brown units within the black layer were noted. These were identified as a potential succession of fires, where the upper unit consists of a white layer overlain by a black layer. This upper black layer is separated from a second black layer below it by a light brown interstratification. The second black layer is further separated from a third black layer by another light brown interstratification. The last black layer contained a thermoaltered and fragmented flint in situ. **Hearth 77** (Fig. 1C) is a pit hearth located between layers X and XI. Micromorphology and magnetic results have been previously described in [Leierer et al. \(2020\)](#) and [Dinçkal et al. \(2024\)](#). Two magnetic hand block samples taken from H77 were processed into thin sections labelled as H77-3 and H77-4.

To assess the magnetic signature of the mentioned structures, paleomagnetic analyses were carried out in the Paleomagnetic Laboratory of the University of Burgos (Spain). 8 oriented hand-block samples were considered for this purpose: 2 blocks from H63, 2 blocks from H66, and 4 blocks from H77. To obtain these samples, plaster was poured over the upper burnt layer. The plaster surface was flattened with the help of a plastic plate and a spirit level. Then, a mark pointing to magnetic North was indicated on the surface, using a magnetic compass. In the laboratory, the blocks were consolidated by immersion in a mixture of sodium silicate and water. After the consolidation, the blocks were cast with plaster and cut in cubic specimens of ~8–10 cm<sup>3</sup>. A selection of specimens with a lesser amount of plaster was made for paleomagnetic analysis. Most of these came from the most superficial and heated part of the blocks (~0–2 cm of depth), with the only exception of a H63 specimen coming from a depth of ~2–4 cm ([Appendix A](#)).

Paleomagnetic analyses on H63 and H66 consisted of thermal demagnetization of natural remanent magnetization (NRM) in 14–19 steps (including the measurement of the original NRM) up to 600–620 °C. It was performed with the help of a paleomagnetic demagnetizer TD48-DC, and the remanence was measured with a superconducting rock magnetometer 2G-755. Additionally, initial magnetic susceptibility (before heating the specimens) was measured with a Kappabridge KLY-4 (AGICO).

Other archived blocks from H63-1 and H63-2, as well as H66-1 were reserved uncut and used for magnetic properties analysis. Magnetic properties measured included low field magnetic susceptibility ( $\chi_{LF}$ ) and progressive acquisition of Isothermal Remanent Magnetization (IRM) and backfield curves (up to 1 T) to obtain the Saturation Isothermal Remanent Magnetization (SIRM) and the remanent coercivity (Bcr), respectively, as well as S-ratio, a measure of the ratio of low-coercive to high-coercive magnetic minerals within a sample ([Bloemendal et al., 1992](#)). Further measurements included hysteresis loops ( $\pm 1$  T) to measure the samples Saturation magnetization (Ms), saturation remanent magnetization (Mrs), and coercivity (Bc). Measurements were taken against depth at resolution of 1 bulk sample (~300 mg) every ca. 5 mm. Furthermore, each block had thermomagnetic curves (up to 700 °C on air; increments of  $\pm 15$  °C/minute) measured at

three locations targeting each microfacies. All measurements were carried out with a Magnetic Measurements Variable Field Translation Balance from the Paleomagnetic Laboratory of the University of Burgos.

Slabs from oriented samples of each hearth were impregnated with epoxy resin at the university of La Laguna, Spain, with thin section grinding conducted at the Wagner Petrographic LLC.

### 3. Results

#### 3.1. Non-archaeological control data

Our observations on the mechanical and field control samples indicate that their optical qualities are indistinguishable, regardless of whether polyester or epoxy is utilized in the re-impregnation process. The most prominent effect of sodium silicate on the optical qualities appears to be the presence of ghostly highlights in the negative void space (Fig. 2A). These are easily identifiable as manufacturing artifacts

because they lie on a different plane than the rest of the sedimentary material. While these shadows are more frequent in sodium silicate-impregnated sections, they are not uncommon in thin section production overall and seem to be a by-product of the glass slide mounting processes. Since they reside on a separate plane, these artifacts do not interfere with the analysis of the thin section. When comparing the samples from Experiment 2, there are no discernible differences in optical qualities between the standard micromorphological samples and those reimpregnated NaSi samples (Fig. 2B and C) either. Samples produced in this quality control test do not provide any evidence against re-impregnating magnetic samples with epoxy or polyester resins. Consolidation with sodium silicate does not inherently compromise the interpretative quality of thin section analysis, as potential artifacts do not seem to affect the sedimentary body itself, thus, they do not diminish the sample's utility in describing the sedimentary sequence.

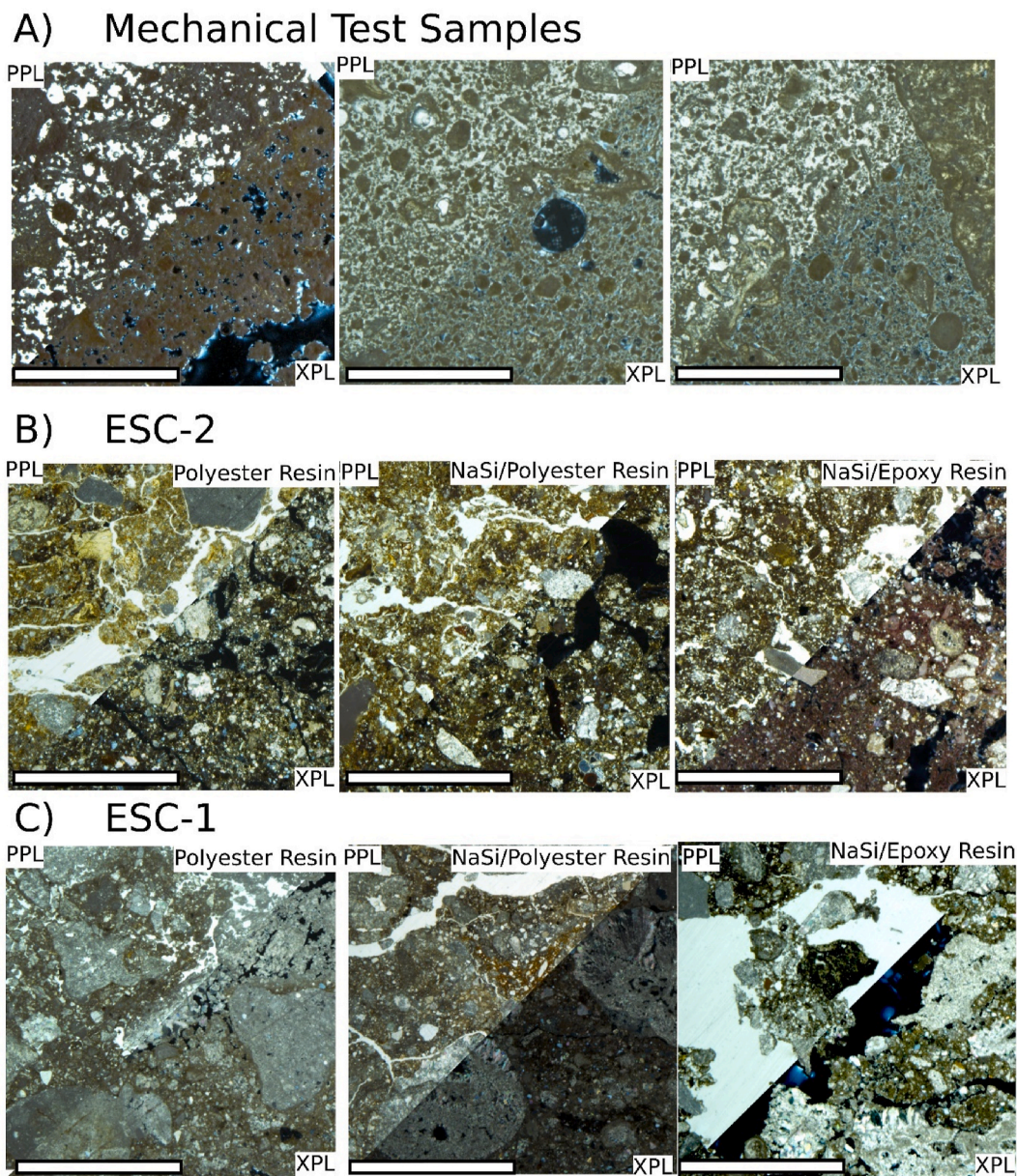


**Fig. 2.** A) Micrographs from samples produced during the mechanical tests. In void space of XPL, ghostly white highlights are grading. B) and C) micrograph from control samples of El Salt. Left: samples impregnated only with polyester resins; Middle: sample impregnated with polyester resin following initial impregnation of sodium silicate resins; Right: Epoxy resin impregnation after initial sodium-silicate impregnation. All scale bars represent 1 mm.

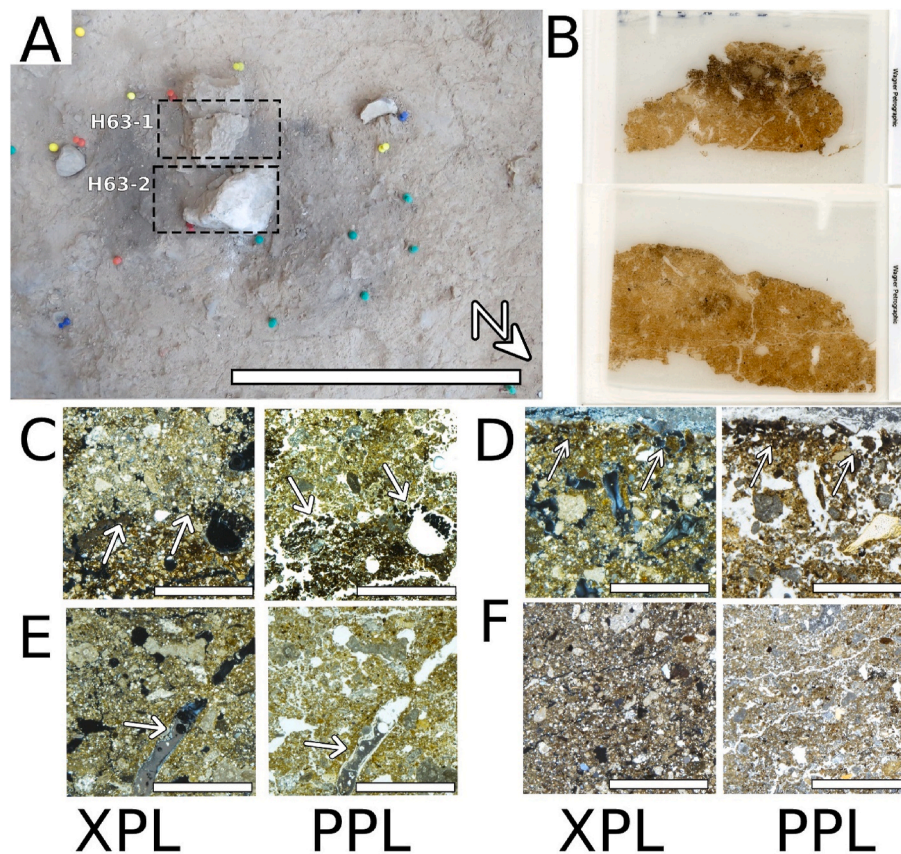


**Fig. 3.** A) Image of H63, showing the approximate location of the magnetically oriented samples. Despite being in the centre, H63-2 is found almost entirely beneath a calcined limestone pebble, which explains the absence of a White Layer (WL) or a well-expressed Black Layer (BL) as it is expressed in sample H63-1 (as seen in panel B). Scale bar represents 30 cm B) Thin sections from H63. Each thin section is  $7.5 \times 5$  cm in dimension. C) Micrograph from H63-1, white arrow shows the interface of the BL and WL. D) Micrograph from H63-2, white arrows show the very thin BL at the top of the thin section (from beneath the burnt limestone rock). E and F) Micrographs highlighting the groundmass of the thermally affected substrata from H63-1 and H63-2, respectively. Of note is the large channel voids present in H63-1 (white arrows). Evidence of bioturbation is present within the thermally affected substrata, while absent in the BL and WL. The presence of bioturbation does not seem to have had a significant impact on the magnetic data, and the absence of such bioturbation in the black or white unit indicates little sediment mixing from combusted units into the thermally affected substrata as root voids were present prior to combustion. Scale bar in Fig. 3C to F represents 1 mm.

### 3.2. Archaeological samples

#### 3.2.1. H63

**3.2.1.1. Micromorphology.** In thin section H63-1, three distinct stratigraphic units were identified. The first, lowest unit exhibited a low organic concentration with coarse, rounded materials, and unburnt bone fragments, primarily occupied with channel voids (Fig. 3D and B). The second unit has a noticeable increase in organic material, a shift towards platy voids and microstructure, enveloping a dark organic matrix. The third unit, characterized by an ash-rich top layer, showed grading from a massive to a platy microstructure, with the presence of ash pseudomorphs and calcite crust (Fig. 3C and B).

Thin section H63-2 shows a single microfacies/domain equivalent to the lowest component in H63-1 (Fig. 3D). A well-formed platy microstructure with a porphyric distribution of coarse and fine materials, including limestone, travertine, and organic bone fragments. Notably, a central region within the sample is richer in organic and clay materials, forming a spherical aggregate with an indistinct boundary. The uppermost part of the deposit featured thin black combusted organic elements (Fig. 3C), which are the only expression of the black facies found in H63-1.

**3.2.1.2. Magnetics.** NRM values of H63 specimens' range between  $1.8 \times 10^{-5}$  and  $3.7 \times 10^{-5} \text{ Am}^2\text{kg}^{-1}$ . Initial magnetic susceptibility values from oriented samples range between  $5.5 \times 10^{-7}$  and  $8.4 \times 10^{-7} \text{ m}^3\text{kg}^{-1}$

(Fig. 7C). Most specimens exhibit  $Q_n$  ratio ( $NRM/H^*Susceptibility$ , where  $H$  = local Earth's magnetic field calculated as 36 A/m; Stacey, 1967; Koenigsberger 1938) values greater than 1.0. Specimens of block H63-1 have very similar NRM, magnetic susceptibility and  $Q_n$  values to each other (Fig. 7C). However, H63-2 shows greater dispersion and a tendency towards lower  $Q_n$  values. In fact, the only H63 specimens with  $Q_n < 1.0$  belong to that block. These differences in  $Q_n$  values seem to come primarily from variability in the NRM, as the susceptibility values of H63-2 are not so different from those of the H63-1 block. Detailed rock magnetic analysis shows a progressive decrease in magnetization with depth (Fig. 4A) which is more pronounced in H63-1 than in H63-2 (See S.I: Detailed Rock Magnetic Data). The magnetization is primarily dominated by low-coercivity minerals, such as magnetite or slightly oxidized magnetite due to maghemitization. We have identified here maghemitization from the Curie temperature of thermomagnetic curves slightly above 580 °C (Fig. 4B–D). This is a common process, in many natural materials related to low-temperature oxidation of magnetite grains, (e.g.: weathering at atmospheric conditions typically below 50 °C) which form an oxidized maghemite shell around an unoxidized magnetite core (O'Reilly, 1984; Özdemir and Dunlop, 1985). In archaeological materials heated to high temperature (>600–700 °C), maghemite can also be formed carrying a full TRM, which is of interest for absolute palaeointensity determinations. Nevertheless, it is a ferri-magnetic (s.s.) mineral and its magnetic properties are very similar to those of magnetite, thus it exhibits a strong magnetic signal (Dunlop and Özdemir, 1997). Its identification in burnt materials is far from

Sample H63-1.B2 (Hearth H63 - Block 1)

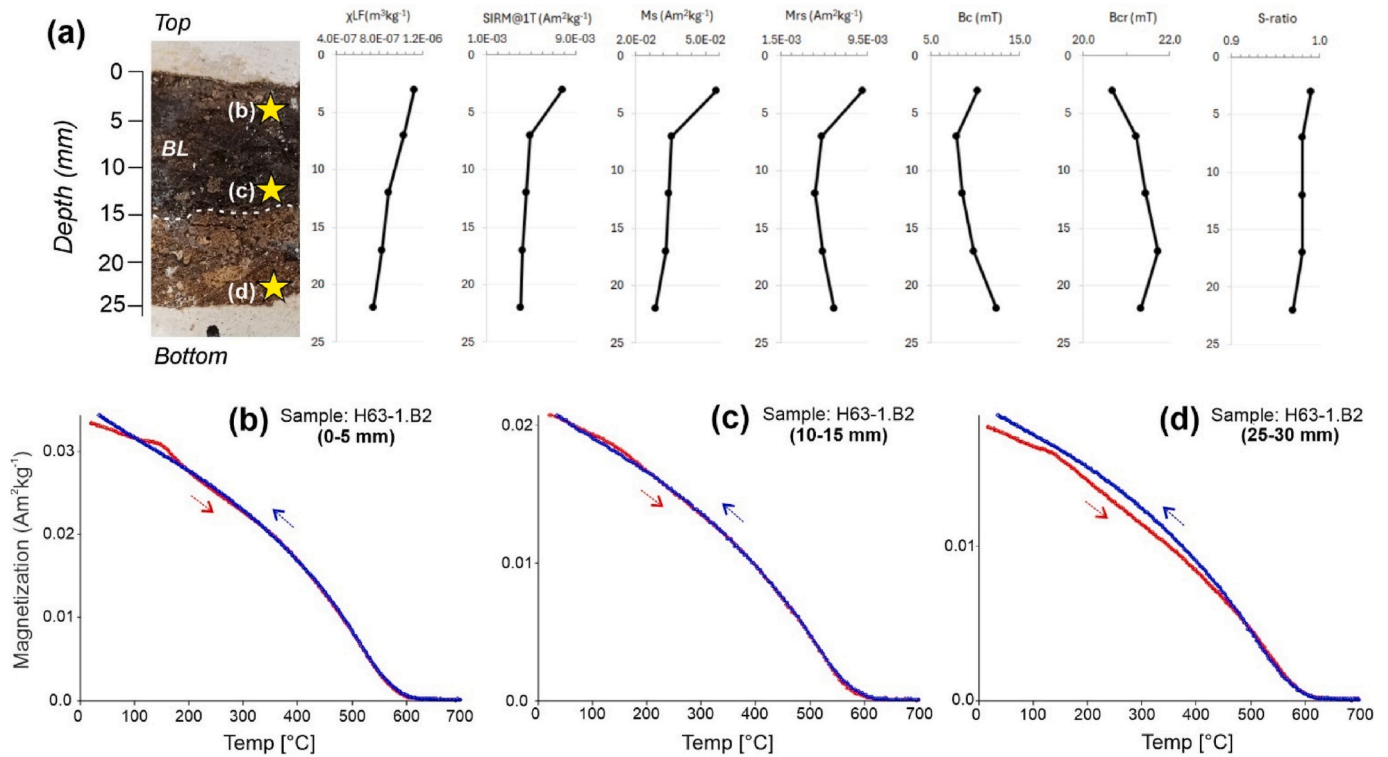


Fig. 4. Magnetic Properties for H63 (block 1). A) Original block subsample with magnetic parameters plotted against depth. Stars denote location of thermomagnetic analysis shown in B-D. Magnetic properties show a reduction in magnetic enhancement with depth while S-Ratios demonstrate that the samples are primarily driven by low-coercive magnetic minerals such as magnetite or maghemite. This is reinforced by thermomagnetic curves which are highly reversible indicating magnetite as the magnetic phase, with some evidence for maghemitization. The lowest sample (thermally affected substrata) is slightly less reversible than B or C, indicating that it was likely less thermally altered.

exceptional (e.g.: Jordanova et al., 2019; 2019), being the cause of distinctive magnetic anomalies. Furthermore, the samples exhibit very high reversibility, suggesting they were subjected to high temperatures ranging from 600 to 700 °C in their initial heating except for the lowest samples (Fig. 4D) which shows somewhat less reversibility.

Regarding the directional analyses, the ChRM direction or component interpreted as that related to last heating (comp. A) was isolated between 200 and 250 °C and 325–585 °C (Fig. 7AI to 7A.IV). Temperature steps below 200–250 °C were excluded to avoid possible viscous influence. In most cases, a high temperature (HT) component was isolated between 350 and 550 °C and 585–620 °C (comp. B; Fig. 7AI, 7A.II and 7A.IV). It is interpreted as the ancient Earth’s magnetic field record prior to the last heating. The stereograms of Fig. 7B and Table 2 show the mean archaeomagnetic directions of both components and their associated statistical parameters according to Fisher’s statistics (1953).

When assessing the ChRM direction of the component A in H63, two different groups of specimens are observed (Fig. 7B; top left panel). Each

population corresponds to a different block. It could suggest some systematic problem during sampling/subsampling. However, when plotting component B, differences between blocks are not so clear (Fig. 7B; top right panel). Apart from this, in one specimen of H63-1, the directions of both components do not follow the trend of the block to which it belongs. This specimen is the only one from a depth of 2–4 cm of the block. Thus, although some sampling/subsampling error cannot totally be excluded in the magnetic data, the differences observed according to the blocks could be related to either the chemical or mechanical properties of specific facies included in each specimen. This could also explain the differences between the NRM values which are driven by the differences in the content of ferrimagnetic mineralogy, with ash having a higher concentration than the black layers while the thermally altered substrata has the lowest. Therefore, the dominant expression of the thermally altered substrata in H63-2 lends itself to significantly lower NRM value. Alternatively, a syn/post-burning chemical process could also be responsible for such directional discrepancies in the component A, as discussed in the following.

3.2.2. H66-1

3.2.2.1. Micromorphology. This study identifies three stratigraphic units within the analysed sample, each characterized by similar material compositions but distinguished by variations in grain size and the concentration of carbonized organic matter. The lowermost unit is a reddish-brown layer with a platy microstructure and a low concentration of organic material, interspersed with charcoal and coarse limestone fragments, as well as both unburnt and partially burnt bone. From bottom to top, this layer grades into a black organic combusted layer. The coarse fraction ranges from sand to gravel size, including major

Table 2

Mean archaeomagnetic directions of the studied hearths and associated Fisher’s statistics parameters (Fisher, 1953). N = number of specimens considered for the calculation of mean direction; N’ = total number of demagnetized specimens; Dec. = declination; Inc. = inclination; k = precision parameter;  $\alpha_{95}$  = semi angle of confidence at 95% probability. Data for H77 are from Leierer et al. (2020).

Hearth/component	N	N'	Dec. (°)	Inc. (°)	k	$\alpha_{95}$ (°)
H63 (comp. A)	10	10	351.2	60.1	4.8	24.7
H63 (comp. B)	8	10	338.8	50.9	7.8	21.2
H66 (comp. A)	9	9	354.1	51.0	10.3	16.9
H66 (comp. B)	9	9	359.6	45.4	3.2	34.4
H77	13	13	352.3	49.3	111.3	3.9

inclusions of bone and charcoal (Fig. 5D). The black layer is marked by a transition into a massive microstructure, with a reduced concentration of coarse grains and an embiggened carbonized organic content. A large, unburnt bone fragment lies between these two layers.

The black layer transitions sharply into a heavily decalcified wood ash unit (Fig. 5B). It has a decreased concentration of organic carbonized material and an increased concentration of calcitic material. This increased calcitic material is associated with an increase in the sand component. In the field, it was noted that there was no distinctive white layer identified, and instead, there were stratifications of what appeared to be light brown units. In the thin section analysis, we find that there is ash, but the ash is likely trampled or at least intermixed with geogenic material that is not a component of the combustion feature. The combustion feature is heavily altered with bioturbation in the form of root voids (Fig. 5C). Along with the high amount of alteration of the top of the combustion feature, the hearth, even if it was once in situ, has been heavily reworked post-depositionally.

**3.2.2.2. Magnetics.** NRM values range between  $2.1 \times 10^{-5}$  and  $6.6 \times 10^{-5} \text{ Am}^2\text{kg}^{-1}$ . Initial magnetic susceptibility analysis of oriented

samples exhibits values between  $3.6 \times 10^{-7}$  and  $1.5 \times 10^{-6} \text{ m}^3\text{kg}^{-1}$  (Fig. 7C). Block H66-1 presents lower susceptibility and NRM values than H66-2. Most specimens exhibit  $Q_n$  ratio values greater than 1.0. In depth rock magnetic analysis reveals little variation across the 30 mm depth analysed (Fig. 6). All samples predominantly contain magnetite, with a Curie temperature near  $580 \text{ }^\circ\text{C}$ , and exhibit very small traces of “maghemitization,” with Curie temperatures around  $600 \text{ }^\circ\text{C}$  (Fig. 6B & D). The exception is the specimen between 15 and 20 mm (Fig. 6C), which clearly exhibits stable maghemite-like with a Curie temperature of  $616 \text{ }^\circ\text{C}$  and is about an order of magnitude more magnetic than the other samples. Given its intense magnetization, which is approximately ten times greater than that of the other samples (Fig. 6A), the possibility of it being a result of relighting cannot be ruled out. This sample is also highly reversible, suggesting it was exposed to high temperatures around  $700 \text{ }^\circ\text{C}$  and correlates with an increased SIRM,  $M_s$  and  $M_{rs}$  values. In contrast, samples in Fig. 6B and D are not reversible; secondary magnetite forms during laboratory cooling, indicating that the samples did not reach the high temperatures ( $600\text{--}700 \text{ }^\circ\text{C}$ ) typically associated with a BL facies (Herrejón-Lagunilla et al., 2019, 2024).

The paleomagnetic component related to the last heating (comp. A) was isolated between  $200 \text{ }^\circ\text{C}$  and  $360\text{--}500 \text{ }^\circ\text{C}$  (Fig. 7AV and 7A.VI). Again, temperature steps lower than  $200 \text{ }^\circ\text{C}$  were excluded to avoid possible viscous influence. A high-temperature component (comp. B), also northward, interpreted as the ancient Earth’s magnetic field record prior to the last heating was isolated between  $400$  and  $550 \text{ }^\circ\text{C}$  and  $600 \text{ }^\circ\text{C}$  (Fig. 7AV and 7A.VI).

The ChRM directions of H66’s components A and B along with their mean archaeomagnetic directions are shown in Fig. 7B (lower panels), and their main statistical parameters according to Fisher’s statistics (1953) are shown in Table 2. Mean directions of both components are considerably scattered ( $k = 10.29$  for comp. A;  $k = 3.19$  for comp. B).

### 3.2.3. H77

Magnetic and micromorphological results from H77 were presented in Leierer et al. (2020) and Dinçkal et al. (2024) and we refer to these papers for an extensive discussion of the data. Table 3 provides a breakdown of the results by microfacies (MF) and their interpretations. It is important to note that the samples from Block H77-3 and H77-4 described in this paper do not correlate with the same designation in Leierer et al. (2020). This discrepancy results from the laboratory pipeline for analysing those samples. In Leierer et al. (2020), the samples corresponding to our Block H77-3 are H77-9 and H77-10, and those corresponding to our Block H77-4 are H77-11 through H77-15. The analysis of these Leierer et al.’s samples show minimal distinction in both rock magnetic parameters and the directional magnetic data.

## 4. Discussion

### 4.1. Mechanical experiments

Micromorphologists are constantly vigilant for potential manufacturing artifacts which can affect analysis. Initial sample extraction, or laboratory handling (Marcazzan et al., 2022) can already cause defects. Improper impregnation can cause crystallization of the resin or formation of voids and bubbles (Stoops 2021), along with grinding errors which can also result in thin sections that are too thin, too thick, or unevenly ground (Marcazzan et al., 2022). In the analysis of Experiment 1 and 2, the focus is not on the sedimentology features of the sample but on the properties of the thin sections itself. The primary consideration is whether any optical artifacts resulting from the NaSi solutions interfere with the analysis in Plane Polarized Light (PPL) or Cross Polarized Light (XPL). Despite the general efforts to minimize manufacturing artifacts in thin sections, eliminating them entirely is not always possible. Nevertheless, to avoid misinterpretation of thin sections, micromorphologists must determine whether the sedimentary features they identify are true representations of the sample or artifacts

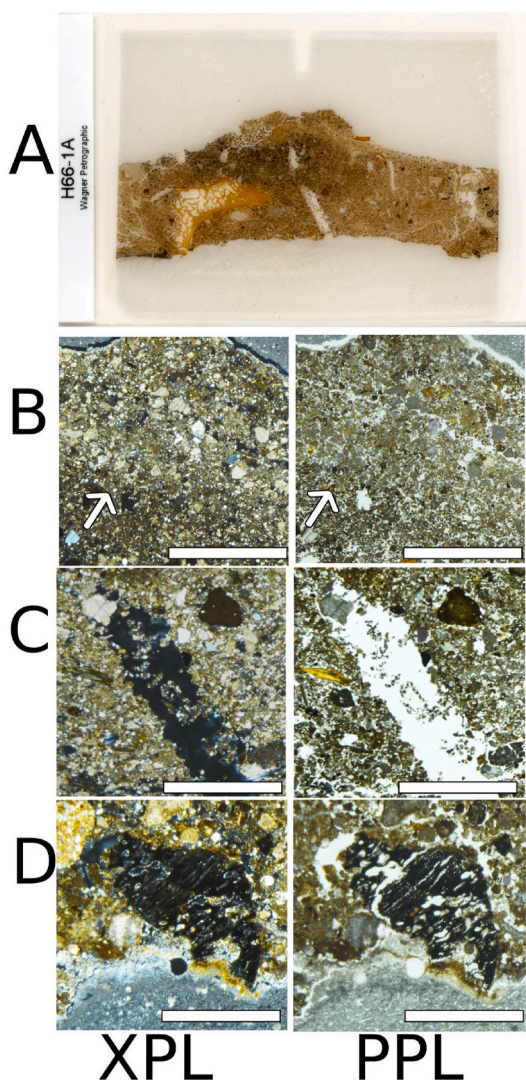


**Fig. 5.** A) Thin section for H66-1. Sample is  $7.5 \times 5 \text{ cm}$ . B-D) Micrographs showing (B) the interface of the black and ash layers present within the sample (white arrow), (C) a channel void intersecting the sample, and (D) a charcoal fragment present within the thermally affected substrata. Scale bars represent 1 mm.

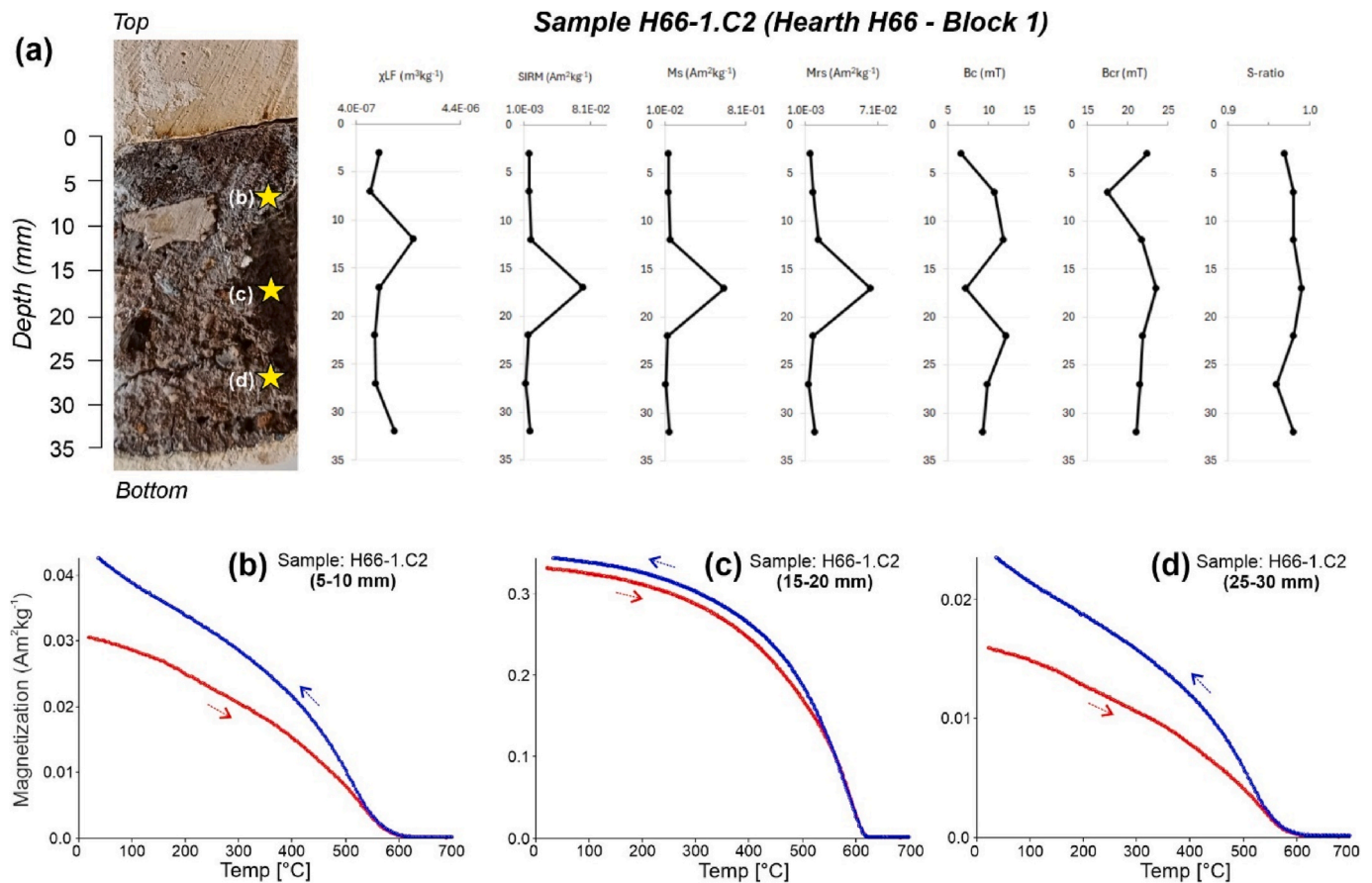


**Fig. 6.** Magnetic Properties for H66. A) Original block subsample with magnetic parameters associated by depth. Stars denote location of thermomagnetic analysis shown in B-D. Samples were consistent in magnetic properties through depth with the sole exception occurring ~15 mm and corresponds with the location of the Black Layer. Thermomagnetic curves are not reversible apart from C which shows a higher degree of reversibility and seems to indicate some thermal alteration.

resulting from its preparation. Therefore, even if the optical qualities of re-impregnated NaSi samples are legible, it is important to understand what artifacts may occur.

While the results for the mechanical experiments demonstrate some manufacturing artifacts which necessitates careful consideration. Corroborative micromorphological samples prepared primarily for that purpose can help control against NaSi influence. However, the lack of such corroborative samples does not invalidate the observations made within NaSi impregnated samples. These sections still offer a comprehensive view of the ground mass, its components, and the different stratigraphic units within the magnetic hand block sample.

## 4.2. Sample discussion

### 4.2.1. H63

Analysis of H63-1 and H63-2 highlights the inconsistencies observed between the magnetic results of the two samples. The burnt layers—identified as black and white layers—are present in H63-1 but notably absent in H63-2, which is primarily the thermally altered substrata. The rock magnetic analysis reveals the primary concentration of ferrimagnetic material (s.l.) is within the black or white layers, with much lower concentrations in the thermally altered substrata unit. Their absence is a discrepancy between the two blocks. The directional results between both blocks are clearly different. This discrepancy corresponds with observations that the primary burning facies, the black and white layers, are either missing or poorly expressed in block H63-2. The variability (scatter) in burning component A across both blocks is likely due to the absence of well-developed burning units in H63-2 sample. The reduced combusted material in H63-2 (Fig. 3B) likely results from the

presence of calcined limestone pebbles at the centre of the hearth. The thermal alteration of this pebble indicates it was present during the main combustion event, thereby providing insulation for the layers beneath the rock and shielding it from the general heating atmosphere of the fire.

The absence or poor expression of these layers could also account for the directional discrepancies between the two sample sets, offset by approximately a 90-degree angle (Fig. 7B - upper left panel), suggesting some form of mechanical deformation in the sedimentary sequence. This deformation is unlikely to stem from a systematic error in measurement, as component B (high-temperature) in both blocks appears consistent (Fig. 7B - upper right panel), indicating that the directional differences in component A between H63-2 and H63-1 likely result from the influence of the rock directly above H63-2. As the rock is burnt, it was likely present during the combustion and would have protected the sediment beneath the rock from some of the influence of the fire, present the formation of black and ash layers, while the weight of the rock may have led to deformation in the more friable surface layers of the deposit, causing the angular difference between burning events. Micromorphological data indicate that the thickness and development of the BL is much lower in block H63-2 (Fig. 3D). Furthermore, specimens from block H63-2 exhibit much lower Qn ratio values than those from block H63-1, some below unity (Fig. 7C). This implies that most specimens of the H63-2 sample do not carry a stable magnetization or, at the very least, their remanence is notably less stable than that of the H63-1 block.

The mean direction of H63-1 is Dec. = 29.6°, Inc. = 36.6°, a95 = 24.6°, k = 15.7, and for H63-2 is Dec. = 283.7°, Inc. = 57.9°, a95 = 12.0°, k = 41.6. This implies an angular deviation = 67.2° between both directions, exceeding the expected dispersion range of the secular variation for mid-latitudes ( $\pm 25^\circ$  in declination and inclination

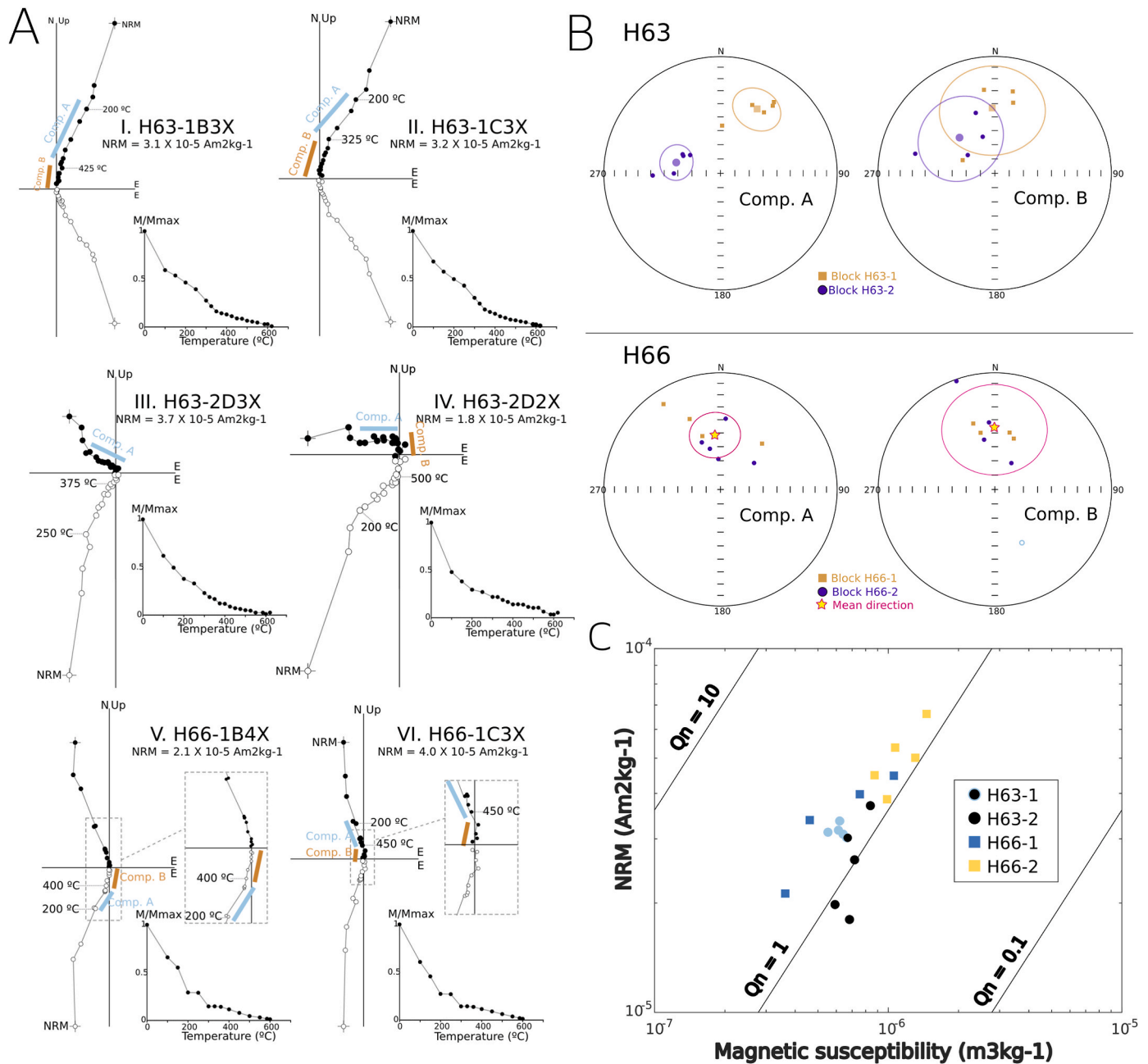


**Fig. 7.** A) Examples of Zijderveld diagrams from H63 and H66 hearths. Solid/open symbols = declination (horizontal plane)/inclination (vertical plane). B) Equal area projection with the mean directions of H63 (up) and H66 (down) components and their respective  $\alpha_{95}$  (semi-angle of confidence at 95% probability). Directions of each individual specimen are also shown. Solid/open symbols = downward/upward. See Table 2 for statistical results. C)  $Q_n$  ratio (Stacey 1967) plot of the specimens of H63 and H66, grouped per block. From right to left, isolines indicate  $Q_n$  values = 0.1, 1 and 10.

oscillating between  $40^\circ$  and  $70^\circ$ ; Molina-Cardín et al., 2018). Therefore, archaeomagnetically speaking it is not strictly “in situ”. The dispersion within a block is small (they are reasonably clustered), but between both blocks is clearly different. If this was due to a mechanical process it would also have affected component B (or high temperature), and this does not seem to be the case. Excluding a sampling error, a plausible option is a chemical process that would have affected exclusively the A component (the one associated with the last heating) during the last heating or time later. Some studies have reported chemical re-magnetisations in directions not parallel to the field direction (e.g.: Özdemir and Dunlop, 1985; Heider and Dunlop 1987). This is obviously a topic that goes beyond the scope of this study. The goal here was not to obtain an archaeomagnetic direction that could be utilized in the reconstruction of the earth's magnetic field, or in studies of secular

variation such as the temporal dissection of paleolithic palimpsests, as Herrejón-Lagunilla et al. (2024) have recently demonstrated. The goal of this analysis is to demonstrate how the combination of micromorphology and archaeomagnetism can effectively identify the formation and alteration processes of Palaeolithic hearths.

#### 4.2.2. H66

The directional magnetic data of H66 indicates that the mean directions for components A and B are notably scattered (Fig. 7B - lower panels). At least one distinctly black burnt layer, approximately 2 cm thick, is identified in the thin section which is further reinforced by rock magnetic data (Fig. 6). While the transition from the substrata to the black unit is gradual, the level of general mechanical alteration on the hearth indicates that the hearth is very poorly preserved. This area of the

**Table 3**

Microfacies breakdown for pit hearth H77. Micromorphological and magnetic analyses conducted in Leierer et al. (2020) (denoted as \* in the table), Dinçkal et al. (2024) (denoted as \*\* in the table), and here agree with each other regarding the interpretation of the hearth. It is an in-situ pit hearth with evidence for multiple burnings, where the combustion events have altered the organic substrate into the red layer with a clear white layer above it. Repeated use is evidenced by both the magnetic parameters and the micromorphological descriptions. For a complete breakdown of the analysis of H77, please refer to the above papers.

Microfacies (MF)	Description*	Magnetic Parameters	Interpretation
MF White Layer (WL)	Above the RL facies, the WL facies are primarily composed of calcitic wood ash. The WL is up to 5 cm thick with a predominantly crumbly or vuggy microstructure, occasionally featuring channels. It is locally fibrous and composed exclusively of wood ash and unidentified plant ash, with few other components besides abundant bone fragments. Burnt bones are integrated within the calcite matrix. This layer includes small amounts of bone, charcoal, and fibrous organics used as fuel sources. Under the microscope in PPL, WL appears pale-yellowish brown, while in XPL, it is locally light grey containing calcium carbonate pseudomorphs likely of wood ash rhombs or bluish-grey zones lacking rhombs with scattered micritic crystals.	Microfacies WL (MFWL) shows the highest values and mean values of magnetic susceptibility ( $\chi_{LF}$ ), NRM, and SIRM, indicating it is the most magnetically enhanced. The white layers are driven by a high concentration of magnetite grains with a large variability of domain structures ranging from dominantly single-domain to dominantly superparamagnetic. The Königsberger (Qn) ratio values consistently exceed unity, showing clear evidence of thermal alteration**. Orthogonal NRM demagnetization diagrams and higher NRM intensities suggest that the WL underwent higher temperatures, generating a higher concentration of ferrimagnetic minerals like magnetite*.	The WL facies represent the final phase of combustion, where most organic materials have been fully burnt to ash. The homogeneity and lack of partially burnt materials suggest a thorough and high temperature burning process. Directional magnetic results indicate that the sample is likely in situ. However, minor aggregates of the red layer present within the white layer indicate that the hearth was burnt multiple times. This is reinforced by some magnetic parameters such as Qn ratios which become stronger at smaller scales of analysis
MF Red Layer (RL)	Directly above the XI facies lies the RL facies, a rubified burnt layer identified in the field. It exhibits a crumbly microstructure and shows a significant reduction in organic content compared to the	Microfacies RL is composed primarily of magnetite, with domain sizes ranging from superparamagnetic with some SD influence to completely SP dominated. Rock Magnetic parameters are generally more enhanced than the XI and weaker than	When examining the transition of the red layer from XI, it becomes apparent that the red layer is a thermally altered variation of the organic substrate. The rubification of the unit is caused by heat alteration, creating high quartz minerals. The general thickness of the unit

**Table 3 (continued)**

Microfacies (MF)	Description*	Magnetic Parameters	Interpretation
	XI facies. The remaining organic components appear as combusted variants of those in XI such as partially burnt or calcined bones. Depending on the position within the feature, the RL is thicker, more reddish, and less organic towards the centre. Towards the edges, it is thinner, with less rubification and slightly increased organic matter. The microstructure and voids resemble those of MFXI. Under the microscope in PPL, RL appears as a massive reddish-brown sediment devoid of organic material, while in XPL, the b-fabric resembles that of MFXI.	those in the WL with Qn ratios indicating thermal alteration within the sample. Initial natural remnant magnetization (NRM) intensities and susceptibility measurements indicate lower ferrimagnetic particle concentrations compared to the WL**. Orthogonal NRM demagnetization diagrams show stable and reproducible directions, with a characteristic remnant magnetization (ChRM) direction isolated between 250 °C and 580–600 °C, suggesting a full TRM (thermoremanent magnetization) and only in one specimen, a pTRM*.	indicates that this process is more intense in the centre. Both rock magnetic parameters and micromorphological evidence suggest that multiple lighting events occurred within the pit hearth, affecting and altering the red layer.
MF XI	Located at the base of the sequence. Visually the layer is relatively undisturbed by heat being rich in organic matter in subangular blocky microstructures. Voids are complex, with channels and chambers. Anthropogenic components such as possible fat-derived char, charcoal, and bone are very abundant. Under the microscope in PPL, MFXI appears dark brown with a brownish-yellow groundmass, with the dark colour due to charcoal and black organic residues. In XPL, the b-fabric is only weakly crystallitic, indicating decalcification.	Rock magnetic parameters show that XI is primarily composed of magnetite with domain sizes varying from Single-Domain (SD) dominant to Superparamagnetic (SP) dominant. XI appear to have less magnetic enhancement compared to RL layers and distinctively less enhancement than WLs. The Königsberger (Qn) ratio values, which exceed unity, imply a thermal origin of magnetization. This microfacies, while less magnetically enhanced, still reflects the general characteristics of the hearth's thermal history**.	Unit XI is the organic substrate present throughout El Salt, and its intense thermal alteration created the Red Layer. The combustion event does not appear to have had an intense impact on what is left of XI, but there is minor evidence of thermal alteration. This is seen in both the partially combusted organic material and in the rock magnetic signature.

site has been noted to be intensely occupied during its the paleolithic period, which may explain the combustion feature's morphology as a product of trampling leading to physical reworking of the hearth in situ. This is reinforced by the high degree of sand that is integrated into the ashy unit (Fig. 5B).

The micromorphological description of H66 is comparable to one of the experimental hearths studied in Herrejón Lagunilla et al. (2019) (NFT9), which was trampled for several days after its extinction. When comparing the directional magnetic data, NFT9's  $k$  or precision parameter ( $k = 79.5$ ) is higher than that of H66 ( $k = 10.3$ ). Such low values for the precision parameter indicate that the material is not well preserved or in situ and one of the processes responsible here for H66 could be trampling. The fact that the scatter is higher in H66 may be an effect of more intensive trampling and/or the effect of other natural taphonomic processes it may have undergone for longer than NFT9 (while NFT9 was excavated 5 years after its extinction, H66 was buried for 52,000 years). Although the mean direction is statistically poor (with a large  $\alpha_{95}$  and very low  $k$ ), it remains northward, suggesting that the disturbance was limited enough to not destroy the hearth completely. Similarly, rock magnetic parameters can be compared. NFT-9 shows significant enhancement in magnetic susceptibility in its black layer, likely due to ash being trampled into the deposit (Herrejón Lagunilla et al., 2019). In comparison, H66 has a spike in magnetic susceptibility at the top of the black layer, at around 13 mm depth (Fig. 6A). This spike in magnetic susceptibility may be due to several reasons. Considering that the mineralogy is dominated by ferrimagnetic minerals (the S-ratio is practically unchanged; Fig. 6A), this susceptibility enhancement could be explained by a general increase in the concentration of finer ferrimagnetic particles which explains the absence of an associated increase in remanence values. It is known that the magnetic susceptibility of ferrimagnetic SP particles at room temperature is very high (Dearing 1999), furthermore archaeological fire ashes contain a significant concentration of SP particles (Peters and Thompson 1999; Carrancho et al. 2009; Jordanova et al., 2019; Dinçkal et al., 2024).

Trampling (or analogous processes) may translocate fine magnetic particles from the highly porous ash into the top of the black layer. This aligns with a trampling interpretation, reinforced by Sossa-Rios et al. (Submitted), who used H66 in an archaeostratigraphic analysis to reveal the area's use as a knapping site postdating the last combustion event, indicated by abundant lithics and a few refits at the top of the black layer. Spikes in some concentration-dependent magnetic parameters (SIRM, Ms or Mrs) lower in the sequence at around 15–20 cm depth, reflect the black layer's own magnetic properties and as stated before, are interpreted as possible evidence of relighting (see the intensity of magnetization in Fig. 6C), which reinforces observations in the field of multiple interstratified black layers—only a single expression of which is present within this sample. Furthermore, there is unmistakable evidence of bioturbation throughout the sample, predominantly within a large channel void filled with insect excrement. These features explain the considerable scatter in the mean direction of the magnetic data while also indicating the disturbances occurred in the hearth's original position, likely indicating a product of trampling. Archaeomagnetic studies at El Salt have utilized the directional record of hearths to dissect the temporality of archaeological palimpsests (Herrejón Lagunilla et al., 2024). The results of this hearth are not viable for that analysis. However, the data itself when combined with micromorphology analysis of the sample can provide qualitative data that can be used to reconstruct taphonomic or anthropogenic processes.

#### 4.2.3. H77

Despite some minor heterogeneity within the samples, magnetic and all micromorphological data from H77 show well preserved combustion features. The analysis of the thin sections conforms with what was identified in Leierer et al. while reinforcing the interpretation of the correlated magnetic data. However, the archaeomagnetic results presented in Leierer et al. (2020) show that one RL specimen (identified as

H77-4 in that paper and coming from archaeomagnetic block H77-1) has an unblocking temperature of around 460 °C, lower than other samples which reached 600–700 °C. It is the only specimen with this behaviour. A thin section from this sample might provide insight into its different magnetic fingerprint which may be a product of many factors such as a heterogenous firing atmosphere in the hearth or variation in the concentration of material within that component of the hearth. Overall, however, H77 provides a cromulent example of a well-preserved combustion feature where the magnetic data, along with the micromorphological analysis of magnetically oriented samples as well as the micromorphological samples are in agreement.

#### 4.3. General discussion on archaeological samples

The original analysis of H77 demonstrate the importance of utilising micromorphology and magnetic analysis to interpret the depositional processes and taphonomy of combustion features (Leierer et al., 2020; Dinçkal et al., 2024). The micromorphological analysis of magnetic samples conducted here further reinforces the potential utility of forming a strong connection between the two methods. While, the additional micromorphological analysis of oriented magnetic samples does not provide deeper insights into the hearth itself. It does provide strong correlation between what is seen in the magnetic data and in the thin section, reinforcing that the natural heterogeneity of the material is not influencing the integration of the magnetic and thin section analysis.

In the analysis of thin sections for samples of hearths H63 and H66, we explore the instances where magnetic samples yield ambiguous data or anomalous records of the Earth's magnetic field direction in the past. The micromorphological examination facilitates the identification of sedimentary characteristics possibly responsible for the anomalous data. This affirms that discrepancies in the data are not attributable to errors in sampling or data integrity but are inherent to the processes which created the deposit as well as the taphonomic processes which altered them after deposition.

It is crucial to underscore that thin section analysis of oriented magnetic samples does not supplant the micromorphological examination of similar features. The comprehensive analysis of sample H77 illustrates the interpretive depth achieved through detailed micromorphological analysis. Nevertheless, micromorphological analysis of the magnetic hand samples serves as an effective method for validating or explaining the magnetic data. This is exemplified by H63, where micromorphological analysis succinctly reveals the discrepancies in the magnetic components between the two blocks by pinpointing the presence or absence of specific sedimentary characteristics which can influence magnetic behaviour. In the case of hearth H66, micromorphological analysis of the hand block reveals that the disparate results stem from the inherently disordered nature of the hearth, rather than from problems in the preparation of the magnetic samples or the measurement process. Thin-section observations corroborate observations in the field regarding the hearths structure. These observations highlighted interlacing light brown units crosscutting the hearths black samples. This corresponds with the reddening of the ash layer through an introduced clay component further highlighting the combustion features altered state. More integrated interdisciplinary analysis of Layer Xb-XI is necessary to establish the degree to the integrity in the archaeological context of these hearths. Our combined approach highlights some degree of physical disturbance, providing further evidence reinforcing field observations of the need of caution in the archaeostratigraphic and spatial analysis of these deposits.

Thin-section examination of oriented magnetic samples should complement, rather than replace, the broader micromorphological analysis of similar features. While the analysis of magnetically oriented thin section acts as a quality control for the magnetic data, especially in situations where micromorphological samples may not capture the entirety of the factors influencing the magnetic readings due to the inherent heterogeneity of anthropogenic features. For example, oriented

magnetic samples sourced from the periphery of the hearth or areas with significant disturbance, such as increased bioturbation, may be reflected in the magnetic data but not in the micromorphological analysis taken from the centre of the hearth, or vice versa. The micromorphological examination of oriented magnetic samples, when juxtaposed to the comprehensive micromorphological analysis, provides a nuanced understanding of the magnetic data as well as providing a simple way to examine more of the feature.

Finally, there is the additional question of the costs versus benefits of conducting micromorphological analysis on magnetically oriented hand blocks. The production of thin sections can be expensive for large scale analysis, with a single standard thin section costing nearly 100 USD commercially, and will take a few months to get a hold of the finished thin section. Recent studies (Herrejón Lagunilla et al., 2024) have demonstrated that archaeomagnetic data can provide unique information for understanding the depositional history of stratigraphic formations. However, this requires well understood magnetic data along with the integrity of its sedimentary context. The ability to contextualize archaeomagnetic and rock-magnetic data, anomalous or otherwise, is crucial to both expediting the analysis of, and accurately interpreting archaeomagnetic material. For the three examples provided in this paper, the micromorphological analysis has provided deeper insight into the magnetic data of the hearths. If the magnetic data are anomalous, the thin section analysis is invaluable in providing the correct context to interpret the magnetic data. Therefore, it makes sense to do the analysis as required. As it stands, the production of magnetically oriented samples already yields slabs as a by-product, and taking magnetically oriented blocks a few centimetres larger than normal will naturally provide a slab which can be utilized to produce thin sections. The only additional step required to preserve that slab is to reimpregnate it with an appropriate amount of epoxy, which is not so expensive. Depending on the magnetic data, along with any hypothetical anomalies present, that preserved slab can then be turned into a thin section as required.

## 5. Summary

This study has demonstrated the feasibility of producing thin sections from magnetic hand block samples previously impregnated with sodium silicate. The use of sodium silicate does not significantly alter the micromorphological structures, aside from sometimes introducing aberrations within void space, which is otherwise not uncommon in micromorphological sample production. This method may not always be necessary for samples with coherent archaeomagnetic data and associated micromorphological samples. However, when samples present anomalous directions, it is invaluable to interpreting the data correctly, as the micromorphological analysis serves as an effective way to discern whether the magnetic data accurately reflects the sedimentary structure being analysed. This merely requires the preservation of a slab from the magnetic hand block, which can be impregnated with either polyester resin or epoxy before being produced into a thin section. At El Salt, the methodology helped interpret anomalous magnetic data from a set of hearths. In hearth H66, the syn- and post-depositional processes appear to be a combination of intense trampling following multiple combustion events as identified through a combination of our method and in-depth rock-magnetic analysis. The study of H63 helped identify structural as well as possible chemical alterations associated with anomalous directional components of the magnetic data. Finally in hearth H77 our analysed reinforced published data by demonstrating that aspects such as bioturbations or other very small-scale processes do not preclude the reliable and statistically robust archaeomagnetic direction. Overall, this integrative method enhances the interpretation of magnetic data, ensuring a more accurate reflection of the sedimentary structure and processes.

## CRedit authorship contribution statement

**Ada Dinçkal:** Writing – review & editing, Writing – original draft, Visualization, Methodology, Investigation, Formal analysis, Data curation, Conceptualization. **Angela Herrejón Lagunilla:** Writing – review & editing, Writing – original draft, Visualization, Methodology, Formal analysis. **Angel Carrancho:** Writing – review & editing, Supervision, Project administration, Methodology, Investigation, Funding acquisition, Formal analysis, Conceptualization. **Cristo M. Hernández Gomez:** Writing – review & editing, Project administration, Methodology, Investigation, Funding acquisition. **Carolina Mallol:** Writing – review & editing, Project administration, Methodology, Funding acquisition, Formal analysis, Conceptualization.

## Declaration of competing interest

None.

## Acknowledgements and Funding

We would like to acknowledge the entire El Salt excavation staff and team members, as well as the Direcció General de Cultura y Patrimoni of the Generalitat Valenciana for the authorization to excavate at El Salt site. Furthermore, we would like to acknowledge the help provided by Aspen Cooper in conception of the original experiments and advice provided during the development of its theoretical frameworks, as well as the work conducted by Amiel Arguinzones in sample preparation and the initial experimentation.

This work was supported by the Municipality of Alcoy, Spanish Government project HAR2015- 68321-P (MINECO FEDER/UE), and a Spanish Government FPI predoctoral grant to A.D. A.C acknowledges the project PID2019105796GB-I00 of the Agencia Estatal de Investigación and Junta de Castilla y León and the European Regional Development Fund (project BU037P23). A. H-L also acknowledges a post-doctoral contract associated with the latter project.

## Appendix A. Supplementary data

Supplementary data to this article can be found online at <https://doi.org/10.1016/j.jas.2024.106081>.

## References

- Bencomo, M., Mayor, A., Sossa-Ríos, S., Jardón, P., Galván, B., Mallol, C., Hernández, C. M., 2023. Use-wear analysis applied in a dissected palimpsest at the Middle Palaeolithic site of El Salt (eastern Iberia): working with lithic tools in a narrow timescale. *Archaeological and Anthropological Sciences* 15 (7), 92. <https://doi.org/10.1007/s12520-023-01787-4>.
- Berna, F., 2017. FTIR microscopy. In: Nicosia, C., Stoops, G. (Eds.), *Archaeological Soil and Sediment Micromorphology*. John Wiley & Sons, Ltd, pp. 411–415. <https://doi.org/10.1002/9781118941065.ch39>.
- Berthold, C., Mentzer, S.M., 2017. X-Ray microdiffraction. In: Nicosia, C., Stoops, G. (Eds.), *Archaeological Soil and Sediment Micromorphology*. John Wiley & Sons, Ltd, pp. 417–429. <https://doi.org/10.1002/9781118941065.ch40>.
- Bloemendal, J., King, J.W., Hall, F.R., Doh, S.-J., 1992. Rock magnetism of Late Neogene and Pleistocene deep-sea sediments: Relationship to sediment source, diagenetic processes, and sediment lithology. *J. Geophys. Res: Solid Earth* 97 (B4), 4361–4375, 10.1029/91JB03068.
- Bradák, B., Carrancho, A., Herrejón Lagunilla, Á., Villalán, J.J., Monnier, G.F., Tostevin, G., Mallol, C., Pajović, G., Baković, M., Borovinić, N., 2020. Magnetic fabric and archaeomagnetic analyses of anthropogenic ash horizons in a cave sediment succession (Crvena Stijena site, Montenegro). *Geophys. J. Int.* 224 (2), 795–812. <https://doi.org/10.1093/gji/ggaa461>.
- Carrancho, Á., Villalán, J.J., Angelucci, D.E., Dekkers, M.J., Vallverdú, J., Vergès, J.M., 2009. Rock-magnetic analyses as a tool to investigate archaeological fired sediments: a case study of Mirador cave (Sierra de Atapuerca, Spain). *Geophys. J. Int.* 179 (1), 79–96. <https://doi.org/10.1111/j.1365-246X.2009.04276.x>.
- Carrancho, Á., Villalán, J.J., 2011. Different mechanisms of magnetisation recorded in experimental fires: archaeomagnetic implications. *Earth Planet Sci. Lett.* 312 (1–2), 176–187. <https://doi.org/10.1016/j.epsl.2011.10.006>.
- Carrancho, Á., Villalán, J.J., Vergès, J.M., Vallverdú, J., 2012. Assessing post-depositional processes in archaeological cave fires through the analysis of

- archaeomagnetic vectors. *Quat. Int.* 275, 14–22. <https://doi.org/10.1016/j.quaint.2012.01.010>.
- Carrancho, A., Herrejón Lagunilla, Á., Vergès, J.M., 2016a. Three archaeomagnetic applications of archaeological interest to the study of burnt anthropogenic cave sediments. *Quat. Int.* 414, 244–257. <https://doi.org/10.1016/j.quaint.2015.10.010>.
- Carrancho, Á., Villalain, J.J., Vallverdú, J., Carbonell, E., 2016b. Is it possible to identify temporal differences among combustion features in Middle Palaeolithic palimpsests? The archaeomagnetic evidence: a case study from level O at the Abric Romaní rock-shelter (Capellades, Spain). *Quat. Int.* 417, 39–50. <https://doi.org/10.1016/j.quaint.2015.12.083>.
- Connolly, R., Jambriña-Enríquez, M., Herrera-Herrera, A.V., Vidal-Matutano, P., Fagoaga, A., Marquina-Blasco, R., Marin-Monfort, M.D., Ruiz-Sánchez, F.J., Laplana, C., Bailon, S., Pérez, L., Leierer, L., Hernández, C.M., Galván, B., Mallol, C., 2019. A multiproxy record of palaeoenvironmental conditions at the Middle Palaeolithic site of Abric del Pastor (Eastern Iberia). *Quat. Sci. Rev.* 225, 106023. <https://doi.org/10.1016/j.quascirev.2019.106023>.
- Dearing, J.A., 1999. Magnetic susceptibility. In: Walden, J., Oldfield, F., Smith, J.P. (Eds.), *Environmental Magnetism: A Practical Guide*, vol. 6. Quaternary Research Association, pp. 25–62.
- Dinçkal, A., Fisher, E.C., Herries, A.I.R., Marean, C.W., 2022. Mapping magnetism: geophysical modelling of stratigraphic features by using in situ magnetic susceptibility measurements at Pinnacle Point 5-6 North, South Africa. *Geoarchaeology* (37), 840–857. <https://doi.org/10.1002/gea.21924>.
- Dinçkal, A., Carrancho Alonso, A., Hernandez Gomez, C.M., Mallol, C., 2024. Magnetic micro-archaeology: a method for conducting rock magnetic microfacies analysis on archaeological soil micromorphology samples, with a case study from El Salt, Alcoy, Spain. *Archaeological and Anthropological Sciences* 16 (3), 44. <https://doi.org/10.1007/s12520-024-01946-1>.
- Dirks, P.H., Roberts, E.M., Hilbert-Wolf, H., Kramers, J.D., Hawks, J., Dosseto, A., Duval, M., Elliott, M., Evans, M., Grün, R., Hellstrom, J., Herries, A.I., Joannes-Boyau, R., Makhubela, T.V., Placzek, C.J., Robbins, J., Spandler, C., Wiersma, J., Woodhead, J., Berger, L.R., 2017. The age of Homo naledi and associated sediments in the Rising Star Cave, South Africa. *Elife* 6, e24231. <https://doi.org/10.7554/elife.24231>.
- Dunlop, D.J., Ozdemir, O., 1997. *Rock Magnetism: Fundamentals and frontiers*. Cambridge University Press.
- Fagoaga, A., Ruiz-Sánchez, F.J., Laplana, C., Blain, H.-A., Marquina, R., Marin-Monfort, M.D., Galván, B., 2018. Palaeoecological implications of Neanderthal occupation at Unit Xb of El Salt (Alcoi, eastern Spain) during MIS 3 using small mammals proxy. *Quat. Int.* 481, 101–112. <https://doi.org/10.1016/j.quaint.2017.10.024>.
- Fagoaga, A., Laplana, C., Marquina-Blasco, R., Machado, J., Marin-Monfort, M.D., Crespo, V.D., Hernández, C.M., Mallol, C., Galván, B., Ruiz-Sánchez, F.J., 2019. Palaeoecological context for the extinction of the Neanderthals: a small mammal study of Stratigraphic Unit V of the El Salt site, Alcoi, eastern Spain. *Palaeogeogr. Palaeoclimatol. Palaeoecol.* 530, 163–175. <https://doi.org/10.1016/j.palaeo.2019.05.007>.
- Fisher, R.A., 1953. Dispersion on a sphere. *Proc. Roy. Soc. Lond. Math. Phys. Sci.* 217 (1130), 295–305. <https://doi.org/10.1098/rspa.1953.0064>.
- Galván, B., Hernández, C.M., Mallol, C., Mercier, N., Sistiaga, A., Soler, V., 2014. New evidence of early Neanderthal disappearance in the Iberian Peninsula. *J. Hum. Evol.* 75, 16–27. <https://doi.org/10.1016/j.jhevol.2014.06.002>.
- Goldberg, P., Berna, F., 2010. Micromorphology and context. *Quat. Int.* 214 (1–2), 56–62. <https://doi.org/10.1016/j.quaint.2009.10.023>.
- Herrejón Lagunilla, Á., Carrancho, A., Villalain, J.J., Mallol, C., Hernández, C.M., 2019. An experimental approach to the preservation potential of magnetic signatures in anthropogenic fires. *PLoS One* 14 (8), e0221592. <https://doi.org/10.1371/journal.pone.0221592>.
- Herrejón-Lagunilla, Á., Villalain, J.J., Pavón-Carrasco, F.J., Serrano Sánchez-Bravo, M., Sossa-Ríos, S., Mayor, A., Galván, B., Hernández, C.M., Mallol, C., Carrancho, Á., 2024. The time between Palaeolithic hearths. *Nature*. <https://doi.org/10.1038/s41586-024-07467-0>.
- Herries, A.I.R., Adams, J.W., 2013. Clarifying the context, dating and age range of the Gondolin hominins and Paranthropus in South Africa. *J. Hum. Evol.* 65 (5), 676–681. <https://doi.org/10.1016/j.jhevol.2013.06.007>.
- Heider, F., Dunlop, D.J., 1987. Two types of chemical remanent magnetization during the oxidation of magnetite. *Phys. Earth Planet. In.* 46 (1), 24–45. [https://doi.org/10.1016/0031-9201\(87\)90169-5](https://doi.org/10.1016/0031-9201(87)90169-5).
- Jordanova, N., Jordanova, D., Mokreva, A., Ishlyamski, D., Georgieva, B., 2019. Temporal changes in magnetic signal of burnt soils – a compelling three years pilot study. *Sci. Total Environ.* 669, 729–738. <https://doi.org/10.1016/j.scitotenv.2019.03.173>.
- Kapper, K.L., Anesin, D., Donadini, F., Angelucci, D.E., Cavulli, F., Pedrotti, A., Hirt, A. M., 2014. Linking site formation processes to magnetic properties. Rock- and archaeomagnetic analysis of the combustion levels at Riparo Gaban (Italy). *J. Archaeol. Sci.* 41, 836–855. <https://doi.org/10.1016/j.jas.2013.10.015>.
- Karkanas, P., Bar-Yosef, O., Goldberg, P., Weiner, S., 2000. Diagenesis in prehistoric caves: the use of minerals that form in situ to assess the completeness of the archaeological record. *J. Archaeol. Sci.* 27 (10), 915–929. <https://doi.org/10.1006/jasc.1999.0506>.
- Karkanas, P., Goldberg, P., 2018. *Reconstructing Archaeological Sites: Understanding the Geoarchaeological Matrix*. John Wiley & Sons Ltd. <https://doi.org/10.1002/9781119016427>.
- Koenigsberger, J.G., 1938. Natural residual magnetism of eruptive rocks. *Terr. Magnetism Atmos. Electr.* 43 (2), 119–130. <https://doi.org/10.1029/TE043i02p00119>.
- Leierer, L., Carrancho Alonso, Á., Pérez, L., Herrejón Lagunilla, Á., Herrera-Herrera, A.V., Connolly, R., Jambriña-Enríquez, M., Hernández Gómez, C.M., Galván, B., Mallol, C., 2020. It's getting hot in here – microcontextual study of a potential pit hearth at the Middle Palaeolithic site of El Salt, Spain. *J. Archaeol. Sci.* 123, 105237. <https://doi.org/10.1016/j.jas.2020.105237>.
- Leierer, L., Jambriña-Enríquez, M., Herrera-Herrera, A.V., Connolly, R., Hernández, C. M., Galván, B., Mallol, C., 2019. Insights into the timing, intensity and natural setting of Neanderthal occupation from the geoarchaeological study of combustion structures: a micromorphological and biomarker investigation of El Salt, unit Xb, Alcoy, Spain. *PLoS One* 14 (4), e0214955. <https://doi.org/10.1371/journal.pone.0214955>.
- Machado, J., Pérez, L., 2016. Temporal frameworks to approach human behavior concealed in Middle Palaeolithic palimpsests: a high-resolution example from El Salt Stratigraphic Unit X (Alicante, Spain). *Quat. Int.* 417, 66–81. <https://doi.org/10.1016/j.quaint.2015.11.050>.
- Machado, J., Molina, F.J., Hernández, C.M., Tarrío, A., Galván, B., 2017. Using lithic assemblage formation to approach Middle Palaeolithic settlement dynamics: El Salt stratigraphic Unit X (Alicante, Spain). *Archaeological and Anthropological Sciences* 9 (8), 1715–1743. <https://doi.org/10.1007/s12520-016-0318-z>.
- Mallol, C., Hernández, C.M., Cabanes, D., Sistiaga, A., Machado, J., Rodríguez, Á., Pérez, L., Galván, B., 2013. The black layer of Middle Palaeolithic combustion structures. Interpretation and archaeostratigraphic implications. *J. Archaeol. Sci.* 40 (5), 2515–2537. <https://doi.org/10.1016/j.jas.2012.09.017>.
- Marczellan, D., Miller, C.E., Conard, N.J., 2022. Burning, dumping, and site use during the Middle and upper Palaeolithic at Hohle Fels cave, SW Germany. *Archaeological and Anthropological Sciences* 14 (9). <https://doi.org/10.1007/s12520-022-01647-7>.
- Marin-Monfort, M.D., Fagoaga, A., García-Morato, S., Ruiz Sánchez, F.J., Mallol, C., Hernández, C., Galván, B., Fernández-Jalvo, Y., 2021. Contribution of small mammal taphonomy to the last Neanderthal occupations at the El Salt site (Alcoi, southeastern Spain). *Quat. Res.* 103, 208–224. <https://doi.org/10.1017/qua.2021.4>.
- Marquina, R., Fagoaga, A., Crespo, V.D., Ruiz-Sánchez, F.J., Bailon, S., Hernández, C.M., Galván, B., 2020. Amphibians and squamate reptiles from the stratigraphic unit Xb of El Salt (Middle Palaeolithic; Alcoy, Spain): palaeoenvironmental and palaeoclimatic implications. *Spanish Journal of Palaeontology* 32 (2), 291–312. <https://doi.org/10.7203/sjp.32.2.17045>.
- Marquina-Blasco, R., Fagoaga, A., Crespo, V.D., Bailon, S., Mallol, C., Hernández, C.M., Galván, B., Blain, H.-A., Ruiz-Sánchez, F.J., 2022. Applying the UDA-ODA discrimination technique to a herpetological association: the case of the Middle Palaeolithic site of El Salt (Alcoi, Spain). *Archaeological and Anthropological Sciences* 14 (7), 139. <https://doi.org/10.1007/s12520-022-01604-4>.
- Massilani, D., Morley, M.W., Mentzer, S.M., Aldeias, V., Vernot, B., Miller, C., Stahlschmidt, M., Kozlikin, M.B., Shunkov, M.V., Derevianko, A.P., Conard, N.J., Wurz, S., Henshilwood, C.S., Vasquez, J., Essel, E., Nagel, S., Richter, J., Nickel, B., Roberts, R.G., Meyer, M., 2022. Microstratigraphic preservation of ancient faunal and hominin DNA in Pleistocene cave sediments. *Proc. Natl. Acad. Sci. USA* 119 (1), e2113666118. <https://doi.org/10.1073/pnas.2113666118>.
- Mayor, A., Hernández, C.M., Machado, J., Mallol, C., Galván, B., 2020. On identifying Palaeolithic single occupation episodes: archaeostratigraphic and technological approaches to the Neanderthal lithic record of stratigraphic unit xa of El Salt (Alcoi, eastern Iberia). *Archaeological and Anthropological Sciences* 12 (4). <https://doi.org/10.1007/s12520-020-01022-4>.
- Mayor, A., Sossa-Ríos, S., Molina, F.J., Pérez, L., Galván, B., Mallol, C., Hernández, C.M., 2022. An instance of Neanderthal mobility dynamics: a lithological approach to the flint assemblage from stratigraphic unit viii of El Salt rockshelter (Alcoi, eastern Iberia). *J. Archaeol. Sci.: Report* 44, 103544. <https://doi.org/10.1016/j.jasrep.2022.103544>.
- Mentzer, S.M., 2017. Micro XRF. In: Nicosia, C., Stoops, G. (Eds.), *Archaeological Soil and Sediment Micromorphology*. John Wiley & Sons, Ltd, pp. 431–440. <https://doi.org/10.1002/9781118941065.ch41>.
- Miller, C.E., Mentzer, S.M., Berthold, C., Leach, P., Ligouis, B., Tribolo, C., Parkinson, J., Porraz, G., 2016. Site-formation processes at Elands Bay cave, South Africa. *South Afr. Humanit.* 29 (1), 69–128.
- Molina-Cardín, A., Campuzano, S.A., Osete, M.L., Rivero-Montero, M., Pavón-Carrasco, F.J., Palencia-Ortas, A., Martín-Hernández, F., Gómez-Paccard, M., Chauvin, A., Guerrero-Suárez, S., Pérez-Fuentes, J.C., McIntosh, G., Catanzariti, G., Sastre Blanco, J.C., Larrazabal, J., Fernández Martínez, V.M., Álvarez Sanchís, J.R., Rodríguez-Hernández, J., Martín Viso, I., García i Rubert, D., 2018. Updated Iberian archeomagnetic catalogue: new full vector paleosecular variation curve for the last three millennia. *G-cubed* 19 (10), 3637–3656. <https://doi.org/10.1029/2018GC007781>.
- Ozán, I.L., Méndez, C., Oriolo, S., Orgeira, M.J., Tripaldi, A., Vázquez, C.A., 2019. Depositional and post-depositional processes in human-modified cave contexts of west-central Patagonia (Southernmost South America). *Palaeogeogr. Palaeoclimatol. Palaeoecol.* 532. <https://doi.org/10.1016/j.palaeo.2019.109268>.
- Özdemir, Ö., Dunlop, D.J., 1985. An experimental study of chemical remanent magnetizations of synthetic monodomain titanomaghemites with initial thermoremanent magnetizations. *J. Geophys. Res. Solid Earth* 90 (B13), 11513–11523. <https://doi.org/10.1029/JB090iB13p11513>.
- Peters, C., Thompson, R., 1999. Supermagnetic enhancement, superparamagnetism, and archaeological soils. *Geoarchaeology* 14 (5), 401–413. [https://doi.org/10.1002/\(SICI\)1520-6548\(199906\)14:5<401::AID-GEA3>3.0.CO;2-A](https://doi.org/10.1002/(SICI)1520-6548(199906)14:5<401::AID-GEA3>3.0.CO;2-A).
- Pérez, L., Hernández, C.M., Galván, B., 2019. Bone retouchers from the Middle Palaeolithic site of El Salt, stratigraphic Unit Xa (Alicante, Spain): first data and comparison with the Middle to upper Pleistocene European record. *Int. J. Osteoarchaeol.* 29 (2), 238–252. <https://doi.org/10.1002/oa.2732>.

- Pérez, L., Machado, J., Sanchis, A., Hernández, C.M., Mallol, C., Galván, B., 2020. A high temporal resolution zooarchaeological approach to Neanderthal subsistence strategies on the southeastern Iberian Peninsula: El Salt stratigraphic Unit Xa (Alicante, Spain). In: *Short-Term Occupations in Paleolithic Archaeology*. Springer International Publishing, pp. 237–289. [https://doi.org/10.1007/978-3-030-27403-0\\_10](https://doi.org/10.1007/978-3-030-27403-0_10).
- Pérez, L., 2023. Subsistencia neandertal en los valles de Alcoi: análisis de los conjuntos faunísticos del yacimiento de El Salt (Alicante), vol. 129. *Museu de Prehistòria de València*. <http://mupreva.org/pub/1617/va>.
- Rampelli, S., Turrioni, S., Mallol, C., Hernandez, C., Galván, B., Sistiaga, A., Biagi, E., Astolfi, A., Brigidi, P., Benazzi, S., Lewis, C.M., Warinner, C., Hofman, C.A., Schnorr, S.L., Candela, M., 2021. Components of a Neanderthal gut microbiome recovered from fecal sediments from El Salt. *Commun. Biol.* 4 (1) <https://doi.org/10.1038/s42003-021-01689-y>.
- Reidsma, F.H., Sifogeorgaki, I., Dinçkal, A., Huisman, H., Sier, M.J., Van Os, B., Dusseldorp, G.L., 2021. Making the invisible Stratigraphy visible: a grid-based, multi-proxy geoarchaeological study of Umhlatuzana Rockshelter, South Africa. *Front. Earth Sci.* 9 <https://doi.org/10.3389/feart.2021.664105>.
- Rodríguez De Vera, C., Herrera-Herrera, A.V., Jambriña-Enríquez, M., Sossa-Ríos, S., González-Urquijo, J., Lazuen, T., Vanlandeghem, M., Alix, C., Monnier, G., Pajović, G., Tostevin, G., Mallol, C., 2020. Micro-contextual identification of archaeological lipid biomarkers using resin-impregnated sediment slabs. *Sci. Rep.* 10 (1) <https://doi.org/10.1038/s41598-020-77257-x>.
- Sossa-Ríos, S., Mayor, A., Sánchez-Romero, L., Mallol, C., Vaquero, M., and Hernández, C. (submitted). The time of the stones: a call for palimpsest dissection to explore lithic record formation processes. *J. Archaeol. Method Theor.*
- Shahack-Gross, R., Shaar, R., Hassul, E., Ebert, Y., Forget, M., Nowaczyk, N., Marco, S., Finkelstein, I., Agnon, A., 2018. Fire and collapse: untangling the formation of destruction layers using archaeomagnetism. *Geoarchaeology* 33 (5), 513–528. <https://doi.org/10.1002/geo.21668>.
- Sistiaga, A., Mallol, C., Galván, B., Summons, R.E., 2014. The Neanderthal meal: a new perspective using faecal biomarkers. *PLoS One* 9 (6), e101045. <https://doi.org/10.1371/journal.pone.0101045>.
- Stacey, F.D., 1967. The Koenigsberger ratio and the nature of thermoremanence in igneous rocks. *Earth Planet Sci. Lett.* 2, 67–68. [https://doi.org/10.1016/0012-821x\(67\)90174-4](https://doi.org/10.1016/0012-821x(67)90174-4).
- Stoops, G., 2021. *Guidelines for Analysis and Description of Soil and Regolith Thin Sections*, vol. 184. John Wiley & Sons Ltd. <https://doi.org/10.1002/9780891189763>.
- Tarling, D.H., 1975. Archaeomagnetism: the dating of archaeological materials by their magnetic properties. *World Archaeol.* 7 (2), 185–197. <https://doi.org/10.1080/00438243.1975.9979632>.
- Tauxe, L., 2010. *Essentials of Rock and Paleomagnetism*. University of California Press. <https://doi.org/10.1525/9780520946378>.
- Tomé, L., Iriarte, E., Blanco-González, A., Jambriña-Enríquez, M., Égüez, N., Herrera-Herrera, A.V., Mallol, C., 2024. Searching for traces of human activity in earthen floor sequences: high-resolution geoarchaeological analyses at an Early Iron Age village in Central Iberia. *J. Archaeol. Sci.* 161, 105897 <https://doi.org/10.1016/j.jas.2023.105897>.
- Vidal-Matutano, P., Henry, A., Théry-Parisot, I., 2017. Dead wood gathering among Neanderthal groups: Charcoal evidence from Abric del Pastor and El Salt (Eastern Iberia). *J. Archaeol. Sci.* 80, 109–121. <https://doi.org/10.1016/j.jas.2017.03.001>.
- Vidal-Matutano, P., Pérez-Jordà, G., Hernández, C.M., Galván, B., 2018. Macrobotanical evidence (wood charcoal and seeds) from the Middle Palaeolithic site of El Salt, Eastern Iberia: Palaeoenvironmental data and plant resources catchment areas. *J. Archaeol. Sci.: Report* 19, 454–464. <https://doi.org/10.1016/j.jasrep.2018.03.032>.
- Weiner, S., Goldberg, P., Bar-Yosef, O., 1993. Bone preservation in Kebara cave, Israel using on-site Fourier transform infrared spectrometry. *J. Archaeol. Sci.* 20 (6), 613–627. <https://doi.org/10.1006/jasc.1993.1037>.
- Weiner, S., Goldberg, P., Bar-Yosef, O., 2002. Three-dimensional distribution of minerals in the sediments of Hayonim cave, Israel: diagenetic processes and archaeological implications. *J. Archaeol. Sci.* 29 (11), 1289–1308. <https://doi.org/10.1006/jasc.2001.0790>.
- Wilson, C.A., 2017. Electron probe X-ray microanalysis (SEM-EPMA) techniques. In: Nicosia, C., Stoops, G. (Eds.), *Archaeological Soil and Sediment Micromorphology*. John Wiley & Sons, Ltd, pp. 451–459. <https://doi.org/10.1002/9781118941065.ch43>.
- Zeigen, C., Shaar, R., Ebert, Y., Hovers, E., 2019. Archaeomagnetism of burnt cherts and hearths from Middle Palaeolithic Amud Cave, Israel: tools for reconstructing site formation processes and occupation history. *J. Archaeol. Sci.* 107, 71–86. <https://doi.org/10.1016/j.jas.2019.05.001>.